3-23-2005

Development and Characterization of Carbon Nanotubes for Sensor Applications

Jessica Eileen Otto
University of South Florida

Development and Characterization of Carbon Nanotubes for Sensor Applications

by

Jessica Eileen Otto

A thesis submitted in partial fulfillment
of the requirements for the degree of
Master of Science in Mechanical Engineering
Department of Mechanical Engineering
College of Engineering
University of South Florida

Co-Major Professor: Ashok Kumar, Ph.D.
Co-Major Professor: Shekhar Bhansali, Ph.D.
Arun Kumar, Ph.D.

Date of Approval:
March 23, 2005

Keywords: electrochemistry, pH, lactate, functionalization, sweat analysis

Acknowledgements

I would like to thank Dr. Ashok Kumar and Dr. Shekhar Bhansali for giving me a chance to work on something outside of my background as an IGERT Fellow. I would also like to recognize Dr. Arun Kumar for providing insight into electrochemistry. This thesis was partially funded by the National Science Foundation IGERT grant DGE Grant No., DGE- 0221681.

I have been lucky enough to stand on the shoulders of giants. For their strong shoulders, I would like to thank my parents. Finally, thank you Justin for being my strongest competition and even stronger supporter. I could not do what I do without you by my side.

Table of Contents

List of Tables

List of Figures

Development and Characterization of Carbon Nanotubes for Sensor Applications

Jessica Eileen Otto

ABSTRACT

The aim of this research was to develop, characterize, and analyze carbon nanotubes as biosensors. In particular, pH and lactate molecules were targeted in this study. The reason these analytes were chosen was twofold. Firstly, when hydrogen ions and lactate are excreted in abnormal amounts in human sweat, they may be an indicator of a separate health problem. Thus, there is a clinical need for such biosensor applications. Secondly, pH and lactate detection represent two different types of electrochemical sensing techniques.

The carbon nanotubes used in this research were single walled and existed in bundles. They were further functionalized with the carboxyl group to detect pH and the enzyme lactate oxidase (LOX) to detect lactate. All carbon nanotube samples were characterized to compare the materials with the attached biomolecules and without the presence of biomolecules. Fourier Transform Infrared Spectroscopy (FTIR) was used to verify the attachment of both the carboxyl group –COOH and LOX to the respective carbon nanotubes samples. Scanning electron microscopy (SEM) was used to analyze the carbon nanotube lactate electrode sample to examine the structure of the electrode.

Both pH and lactate biosensors were used in a standard three electrode electrochemical cell where the carbon nanotubes behaved as the working electrode with

an Ag/AgCl reference electrode and a platinum wire as the counter electrode. Each sample was separately interrogated by several voltammetry techniques such as linear, cyclic, and square wave. Square wave voltammetry proved to be the best template to use to sense the target analytes. The functionalized CNT-COOH electrode displayed a linear response to pH 1-10, with a negative voltage shift corresponding to an increase in pH. Two types of lactate sensors were fabricated, both of which exhibited an increase in current corresponding to an increase in lactate concentration. The functionalized CNT-LOX on a glassy carbon electrode displayed an amperometric response in the range of 1 mM – 4 mM lactate. The CNT-LOX on a Si/ITO substrate displayed an amperometric response in the range of 0.01 M – 0.05 M lactate.

Chapter One

Introduction

In 1959 physicist Richard Feynman challenged the scientific community to learn how to manipulate and control the atom to make very small things [1]. Thirty-two years later, carbon nanotubes (CNTs) were discovered [2]. This has created a flurry of research at nanoscale. Carbon nanotubes have since been the focus of research groups due to their unique mechanical and electrical properties that far exceed all other known materials. They possess a Young's Modulus higher than diamond, on the order of about 0.64 TPa [3], can behave as either a metallic or a semiconductor material [4], and have band gaps that depend specifically on the structure of the nanotube [5].

Several versatile applications of carbon nanotubes have been proposed. The mechanical robustness of carbon nanotubes lends them to behave ideally as scanning probe tips for atomic force microscopy. The small tube diameter and cylindrical shape allow for imaging of deep crevices and improved resolution [6]. Carbon nanotubes also have a high aspect ratio which makes them good candidates for field emission electron sources with an increased emission rate based on an open CNT tip [7]. Another potential application is in the field of electrochemistry. The low resistivity and high surface area of carbon nanotubes makes them an ideal electrode material. Single-walled carbon nanotubes (SWNTs) have the largest surface area to volume ratio of any carbon material, 3000 m^2/g, as all their atoms are on the surface [8].

The following research focuses on the development of carbon nanotube-based biosensors for detecting analytes in human sweat. Sweat contains electrolytes and minerals that, when exhibiting abnormal amounts, are useful diagnostic tools for other health problems. In this work, carbon nanotubes have been used as electrochemical sensors for the detection of such analytes. To date, there are no carbon nanotube biosensor arrays that simultaneously detect analytes in sweat. As a diagnostic or continuous monitoring tool, a small noninvasive sweat biosensor has great potential. The successful fabrication of a carbon nanotube pH sensor and lactate sensor has been achieved. Single-walled carbon nanotubes (SWNTs) were properly functionalized to be specific to either pH or lactate concentration when applied in a phosphate buffer solution. As well as electrochemical characterization, the SWNTs were also characterized with Fourier transform infrared (FTIR) spectroscopy and scanning electron microscopy (SEM).

The carbon nanotubes behaved as the working electrode in a standard three-electrode electrochemical cell. The functionalized CNTs exhibited a voltammetric response to shifts in pH of the buffer solution with very high sensitivity. When placed in varying concentrations of lactate solutions, the modified nanotubes responded with an amperometric response to changes in lactate concentration.

This work will begin with a general discussion on biosensors and electrode material selection, in particular for skin and sweat analysis. Carbon nanotube properties and growth processes will be introduced in order to provide a background for further explanation of CNT functionalization and electrode fabrication techniques. The experimental electrode design process will be detailed for both pH and lactate sensors,

followed by a discussion on CNT characterization. Finally, a discussion and interpretation of the pH and lactate sensor results will conclude as well as suggestions for future work.

Chapter Two

Biosensor Applications and Material Selection

2.1. Biosensor Applications

Biosensor technology has grown at such a rapid rate that several new sensors used to interrogate the human body have been developed and today are in high demand. Overall, this situation has created a rapidly rising demand for new noninvasive and in vitro sensor technologies to speed up testing. Two categories of biosensors have emerged: point-of-care sensors [9] and wearable sensors [10]. An example of both types of biosensor applications will follow.

2.1.1. Point-of-Care Sensors

Point-of-care sensors can measure analytes in the human body through blood, saliva, urine, and sweat mediums. They are usually meant for one-time diagnostic use. One common sensor of this type is discussed below.

2.1.1.1. Alcohol Sensor

One of the most commonly used noninvasive biosensors of this type is used to measure saliva alcohol concentration. Alcohol sensors can consist of an oxygen electrode or an amperometric hydrogen peroxide electrode. When these sensors are functionalized with the enzyme alcohol oxidase, the following chemical reaction occurs:

$$\text{Alcohol} + O_2 \xrightarrow{alcohol\_oxidase} H_2O_2 + \text{Acetaldehyde}$$

The alcohol is assayed by measuring the decrease in oxygen with an oxygen electrode or by measuring the increase in hydrogen peroxide with a hydrogen peroxide electrode [9].

2.1.2. Wearable Sensors

Wearable biosensors are used when continuous monitoring of an analyte is needed. While a glucose sensor is described below, other wearable sensors would include a pulse monitoring sensor and a blood oxygen sensor.

2.1.2.1. Glucose Sensor

Monitoring of blood glucose is a crucial reality of managing diabetes. However, even a minimally invasive technique involves pricking the fingers several times per day and impedes on the quality of life of a person living with diabetes. The GlucoWatch automatic glucose biographer (Cygnus Inc, Redwood City, Calif.) provides a noninvasive means to measure glucose levels for as long as 12 hours after one single blood glucose calibration [10]. The noninvasive method utilized by the GlucoWatch extracts glucose through the skin using an applied potential (a process known as iontophoresis) and measures the extracted sample using an electrochemical-enzymatic sensor. Iontophoresis is a technique whereby a constant, low-level electrical current is conducted through the skin between an anode and cathode. The glucose sensor relayed an electrochemical amperometric response in relation to glucose concentration. The sensor achieves sensitivity by using the enzyme glucose oxidase (GOX), which only reacts with glucose. The following chemical reaction occurs:

$$\text{Glucose} + O_2 \xrightarrow{GOX} \text{Gluconic acid} + H_2O_2$$

Furthermore, hydrogen peroxide is oxidized as follows:

$$H_2O_2 \rightarrow O_2 + 2H^+ + 2\ e^-\text{'s}$$

The sensor works by measuring how many electrons are transferred to the working electrode: in this case, one molecule of glucose is extracted through the skin for every two transferred electrons.

2.2. Sweat Analyte Sensors

An understanding of basic skin and sweat terminology is needed prior to the development of any sensor meant to noninvasively measure analytes in the sweat or on the skin surface.

2.2.1. Skin and the Sweat Glands

Human skin is the largest organ system of the body and constitutes 15% to 20% of total body mass. Its functions include thermoregulation, protection against dehydration, to serve as a barrier to pathogens and ultraviolet radiation, collection of sensory information, and to synthesize Vitamin D. The skin is divided into three unique sections: the epidermis, dermis, and subcutaneous layer (see Figure 2.1). The outermost layer of the epidermis is called the stratum corneum and is the final destination of the sweat glands.

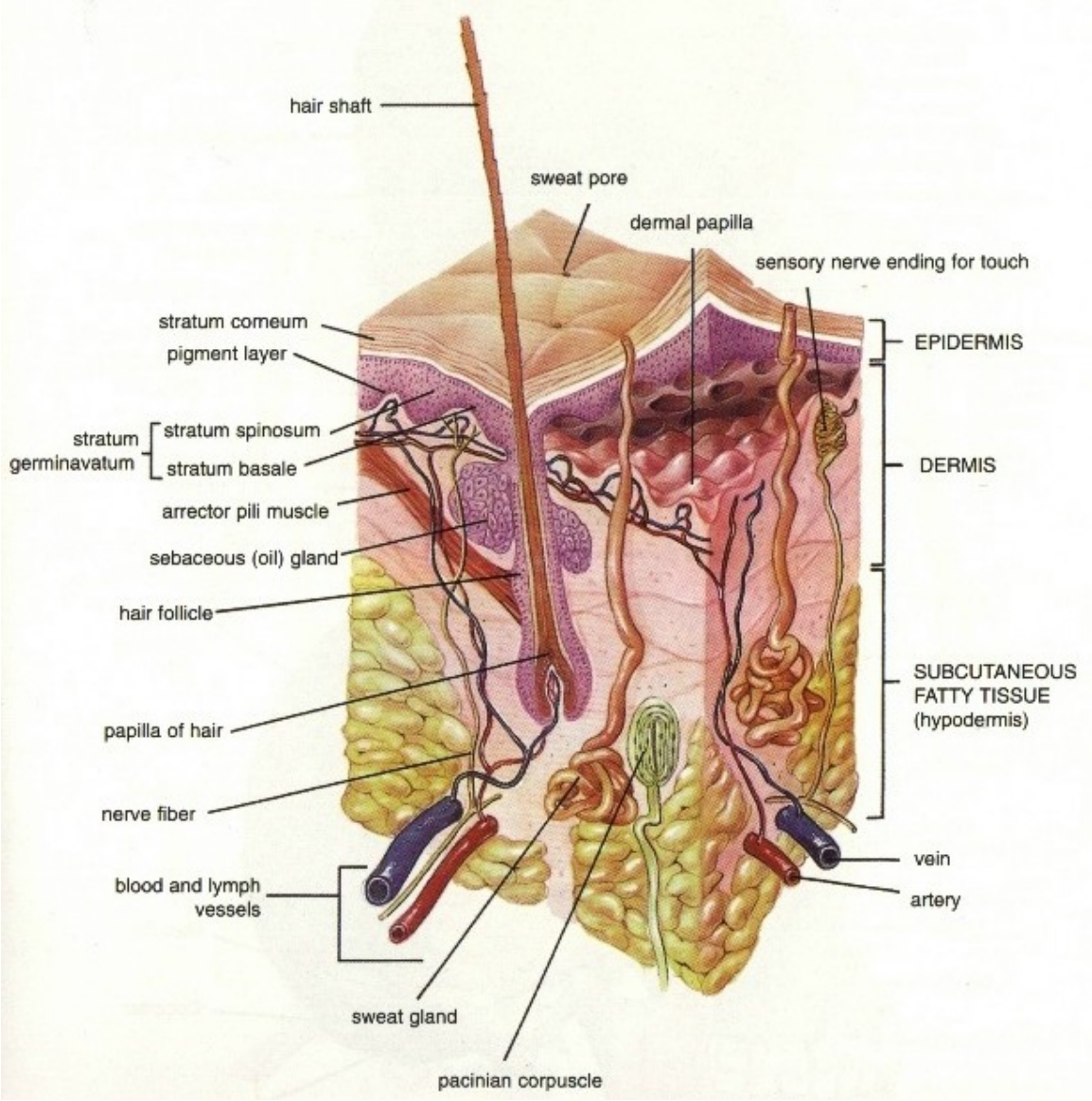

Figure 2.1. Cross-section of human skin.

The sweat glands (also called sudoriferous glands) originate in the dermis and subcutaneous layer of the skin. There are two types of sweat glands: apocrine and eccrine. Apocrine glands open onto the hair follicle. They are found primarily in the armpits and groin area. Apocrine glands secrete through an associated hair follicle in response to stress and sexual stimulation. They secrete odorless fluid that acquires odor

from bacterial decomposition. Eccrine glands are separate from hair follicles, and arise directly from the subcutaneous tissue to the skin surface. They are composed of simple, coiled, tubular glands and ducts that open onto the skin surface. The sweat that is secreted is a mixture of water, salt, urea, ammonia and uric acid. From this point on, the sweat produced only from eccrine glands will be discussed.

The skin is slightly acidic due to the acid mantle which exists on top of the stratum corneum. The acid mantle is a protective layer that wards off non-resident bacteria. A slightly acidic pH of the skin (4-6) helps deter colonization by non-resident bacteria and pathogens because many bacteria can survive only in a narrow pH range near neutral. The pH of skin is contributed by the sweat glands, sebum, and any waste product from the resident skin bacteria that mix together on the skin surface. If the acid mantle is lost or disrupted, the skin becomes more prone to damage and infection.

2.2.2. The Natural Moisturizing Factor

The natural moisturizing factor (NMF) is made up chiefly of amino acids and their metabolites, lactate and inorganic ions such as potassium, sodium, and calcium. Several reports have suggested the important role of amino acids in influencing the state of hydration in the stratum corneum [11, 12]. Nakagawa et al. [13] studied the relationship between the NMF (in particular lactate and inorganic ions) and its association to the physical structure of the stratum corneum. Their results confirmed significant decreases in the lactate and potassium content from summer to winter (see Figures 2.2 and 2.3), as well as correlations of both lactate and potassium levels with

three physical properties of the stratum corneum. Further, potassium lactate restored the hydration of forearm stratum corneum after the NMF had been extracted [13].

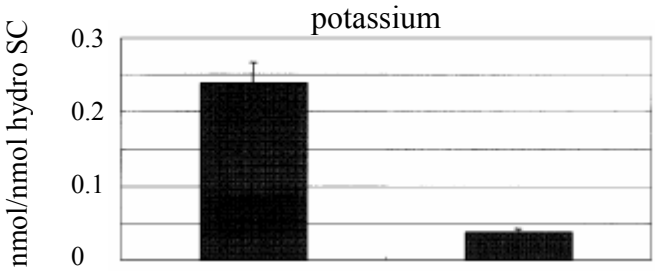

Figure 2.2. Level of potassium in NMF change between winter and summer [13].

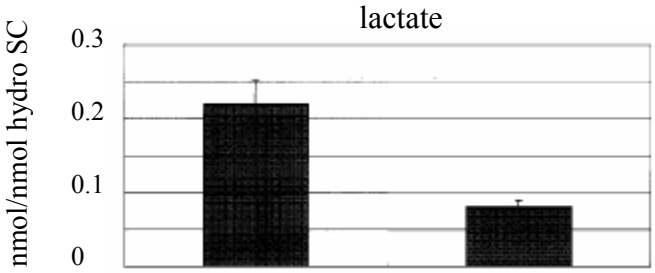

Figure 2.3. Level of lactate in NMF change between winter and summer [13].

2.2.3. Composition of Human Sweat

Sweat consists primarily of electrolytes (Cl^-, Na^+, K^+) as well as compounds such as lactate and ammonia. Abnormal levels of some of these ions or compounds may have a direct relationship with a separate health issue. While this research covers the pH and lactate sensor fabrication, a brief description of the importance of each ion in sweat will follow as a motivation for future work.

Cystic fibrosis (CF) is the most common genetic disease in the United States, occurring in approximately 1 out of every 3000 live births [14]. CF manifests itself with

an increase in both sodium and chloride sweat concentrations. It causes the exocrine glands, which produce mucus and sweat, to produce abnormal secretions. A sweat collection is usually taken on the forearm and analyzed to diagnose the disease.

While potassium plays an important role in hydration and stiffness of the stratum corneum (see Section 2.2.2.), it also serves very important roles inside the body. Small changes in the potassium that is present outside the cells can have severe effects on the heart, nerves, and muscles. Low potassium level is known as Hypokalemia. Usually the kidney controls the potassium balance in the body; however, with the onslaught of Hypokalemia, there is a dysfunction in the normal process and the rapid loss of urine or sweat without the sufficient replacement of potassium occurs. Hypokalemia is an indicator that another disease that may be affecting the body, such as kidney disorders, magnesium deficiency, leukemia, and congestive heart failure.

Sweat lactate is a function of sweat gland energy metabolism. Because lactate is a product of the sweat gland itself, a decrease in oxygen supply induces a rise in sweat lactate concentration and a decrease in sweat gland activity. For example, pressure applied to soft tissue will cause a rise in sweat lactate concentration with respect to the rest of the body's sweat lactate concentration. The development of pressure sores, or bedsores, has implications on the health of a bedridden individual as well as requirements for health care professionals.

Ammonia, a waste product, when excreted in the sweat can be an indicator of several biological occurrences. People who intake more animal protein than usual, such as those on the Atkin's diet, will excrete increased levels of ammonia in the sweat. Continuous measurement of ammonia could aid in exercise and dietary plans for those

individuals. Excessive ammonia excretion may also be an indicator of a disease associated with protein degradation, such as kidney or liver malfunction.

2.2.4. Material Selection for Sweat Analyte Analysis

Previous biosensor research has focused on the fabrication of a sensor utilizing micro-electromechanical systems (MEMs) technology and a conducting polymer film [15]. However, carbon nanotubes are gaining more recognition as a stable electrode material that is not reduced or oxidized over a substantial range of potentials [8]. A review of these two types of electrode material will follow as well as a discussion on the advantages and disadvantages of each.

2.2.4.1. Polymer Electrodes

Lakard et al. [15] developed a potentiometric pH sensor based on platinum electrodes modified with two synthetic enzymes and biocompatible polymer thin films: linear polyethylenimine (L-PEI) and linear polypropylenimine (L-PPI). The chemically modified electrodes showed a linear behavior from pH 3 to 10 during 30 days. In order to miniaturize this sensor, a photolithography process was used to pattern metal electrodes on top of an oxidized silicon wafer (see Figure 2.4) [15]. The electrodes were also interdigited to increase the contact surface between the electrode coated with the polymer and the analyte (see Figure 2.5). The potentiometric response of the microsystem appeared linear to pH changes from pH 4 to 10 [15].

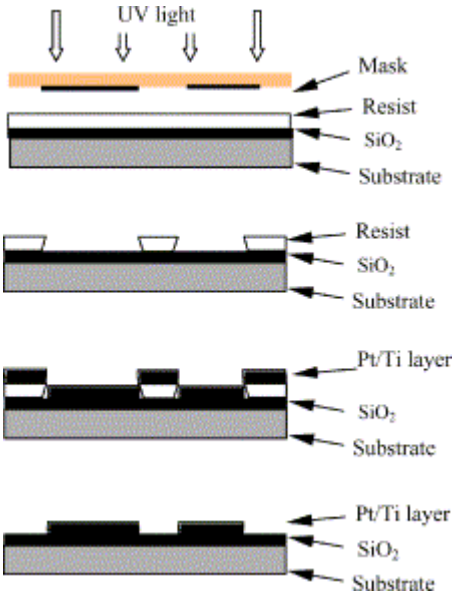

Figure 2.4. Principle of lift-off process used for biosensor fabrication [15].

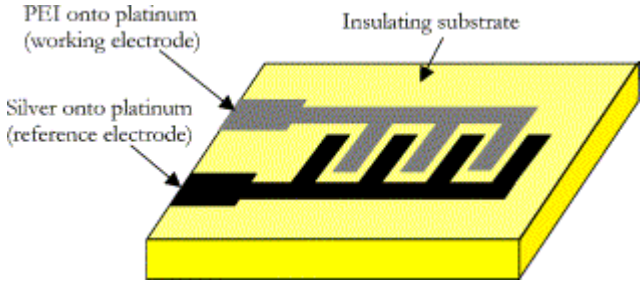

Figure 2.5. Schematic drawing of interdigited microelectrode array [15].

One advantage of using a polymer thin film as in [15] is ease of application on an electrode surface. However, the L-PEI and L-PPI modified pH microelectrode array did not demonstrate as much sensitivity or shelf life as the larger modified platinum electrodes. The decrease in sensitivity may have been due to the silver layer used as the reference electrode in the miniaturized biosensor [15].

2.2.4.2. Carbon Nanotube Electrodes

Electron transfer reactions occur when carbon nanotubes are modified with a functional group or enzyme. Due to their sensitivity and nanoscale size, carbon nanotube biosensors provide great potential for the real time detection of a wide range of biomolecules. Hu et al. [16] modified carbon nanotubes with a functional group and the result was that the ends of CNT were opened and oxidized into carboxylate groups, which may react with other reagents. The carboxyl-modified CNT film electrodes showed stable cyclic voltammetric behavior in 1 mM Fe^{2+} / 0.2 M $HClO_4$ solution involving the reduction of the carboxylic acid groups on the CNTs [16]. Immobilization of proteins on the sidewalls and open tips of carbon nanotubes also results in very sensitive nanosensors [17]. Besteman et al. [17] demonstrated the first biosensor based on an individual SWNT (see Figure 2.6). Immobilization of the enzyme GOX decreased the conductance, which can be attributed to a change in the total capacitance of the tube. Changes of conductance of the GOX-coated semiconducting SWNTs upon addition of glucose indicated that an enzyme-activity sensor can be constructed at the single molecule level of an individual SWNT.

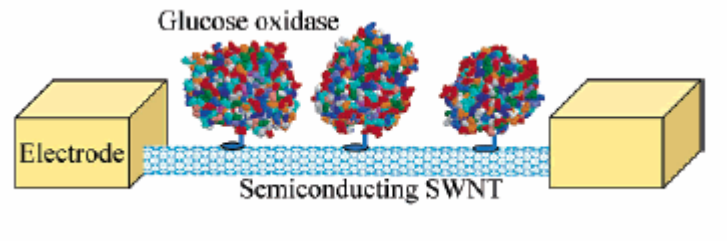

Figure 2.6. Schematic drawing of two electrodes connecting a semiconducting SWNT with GOX enzymes immobilized on the surface [17].

Carbon nanotubes have a high aspect ratio which leads to a much larger surface area than conventional electrodes such as the glassy carbon electrode. A single nanotube probe has huge potential in the development of individual nanoprobes and sensing at the molecular level. They are able to detect low level concentrations and respond well to electrochemical characterization. Carbon nanotube electrodes demonstrate catalytic activities towards many electrochemical reactions [18]. As electrode materials, carbon nanotubes show better behavior than traditional carbon electrodes, including a good conducting ability and high chemical stability.

Chapter Three

Carbon Nanotube Properties and Growth Processes

3.1. Carbon Nanotube Properties

An ideal carbon nanotube can be viewed as a hexagonal network of carbon atoms rolled up to form a seamless, hollow cylinder. Only a few nanometers in diameter, the shaft can grow to be several microns long. The end of the nanotube is capped off with one half of a fullerene molecule. A single-walled carbon nanotube (SWNT) is one single rolled up graphite sheet, whereas a multi-walled carbon nanotube (MWNT) consists of several concentric cylinders of SWNTs. A SWNT is based on a two-dimensional graphene sheet and can be characterized by a chiral vector **C**. The chiral vector is defined on the hexagonal lattice as $\mathbf{C} = n\mathbf{a}_1 + m\mathbf{a}_2$, where $\mathbf{a}_1$ and $\mathbf{a}_2$ are unit vectors, and n and m are integers. The chiral angle, θ, is measured relative to the direction defined by $\mathbf{a}_1$ (see Figure 3.1). When a graphene sheet is rolled up to form the cylinder, the ends of the chiral vector meet each other and connect two crystallographically equivalent sites [19]. Thus, the length of the chiral vector is equal to the circumference of the nanotube.

3.1.1. Electrical Properties

When a graphene sheet is 'cut' and rolled up, the chiral vector defines one of three different possible nanotube structures. Depending on (n,m), these structures are: armchair, zigzag and chiral nanotubes (see Figure 3.2).

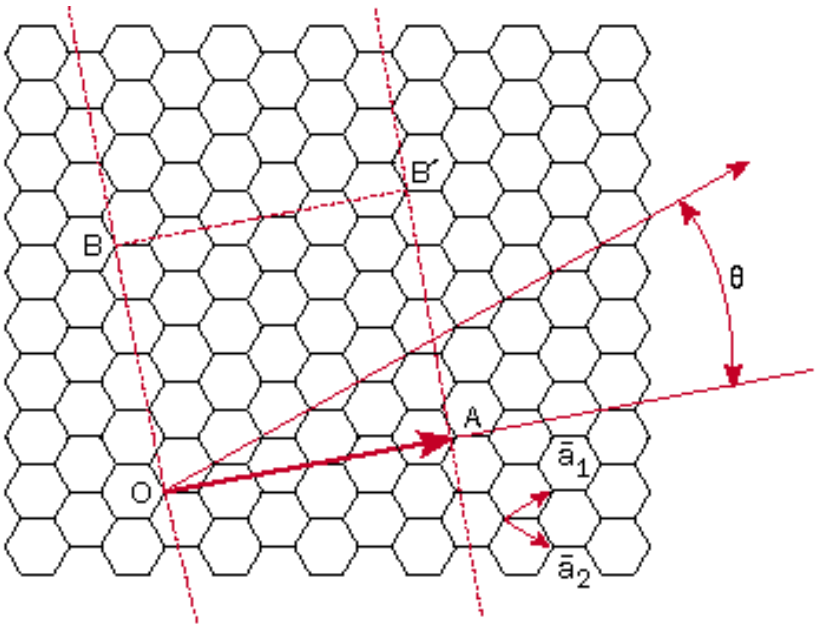

Figure 3.1. A two-dimensional graphene sheet defines a chiral vector, **OA**, and a chiral angle θ with respect to the zigzag axis [19].

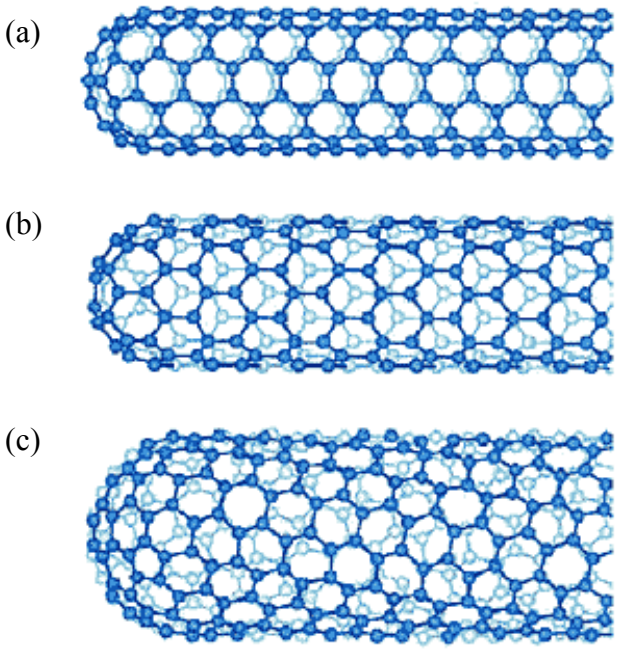

Figure 3.2. Three nanotube structures: (a) armchair, (b) zigzag, and (c) chiral [20].

Armchair nanotubes form when n = m and the chiral angle is equal to 30°. Zigzag nanotubes form when n equals zero or m equals zero and the chiral angle is equal to 0°. All other nanotubes are called chiral nanotubes and form when the chiral angle is between 0° and 30°. The values of (n,m), which govern the diameter and the chirality of the tube, will determine whether the carbon nanotube will behave as a metallic or semiconductor material. A carbon nanotube will behave as a metallic when n is a multiple of three [21]. All armchair nanotubes are metallic, as well as one-third of all zigzag nanotubes (see Figure 3.3).

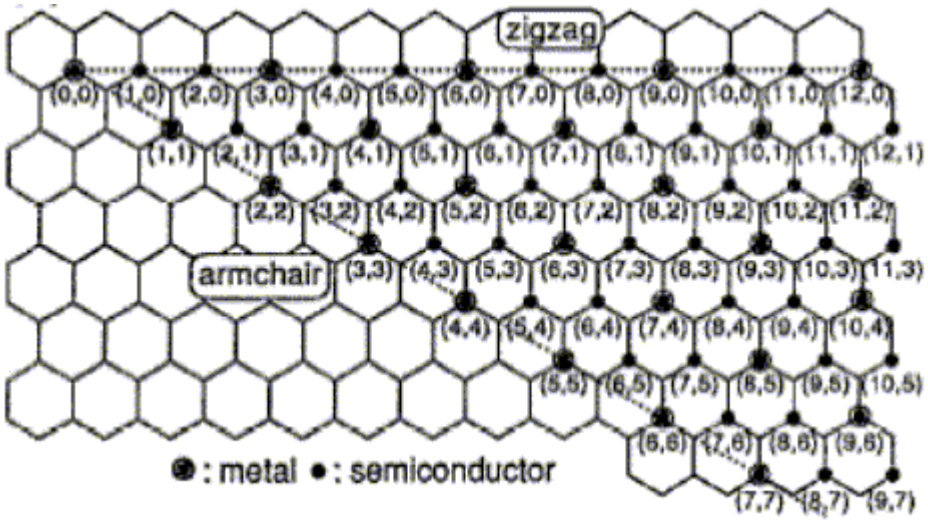

Figure 3.3. Electronic properties determined by (n,m) [21].

Regardless of whether a carbon nanotube behaves as a semiconductor or a metal, the chemical bonding between the carbon atoms remains unchanged for each case. This result is due to the unique structure of a two-dimensional graphene sheet, which is a semiconductor with a band gap of zero. The band gap approaches zero at large diameters

of nanotubes as for a graphene sheet because in a nanotube behaving as a semiconductor the band gap is inversely proportional to the tube diameter.

3.1.2. Mechanical Properties

In 1991 it was reported that when fullerene molecules were collided against graphite and silicon over a wide range of energies that the events were highly inelastic and nonfragmenting [22]. This same property of resilience becomes magnified with a carbon nanotube. Due to its extremely small structure, experimental measurements of mechanical properties of carbon nanotubes such as Young's modulus and tensile strength have been a challenge. The first experimental data of the Young's modulus occurred by isolating a carbon nanotube and measuring the amplitude of its intrinsic thermal vibration in a transmission electron microscope [23]. The thermal vibration at the free ends of the nanotubes was a function of temperature and Young's modulus. Assuming the nanotube behaved as a straight cantilever rod with one end fixed and the other vibrating, an average value of 1.8 TPa for the Young's modulus was obtained.

The atomic force microscope (AFM) has also been applied to measure the mechanical properties of a carbon nanotube. A carbon nanotube was pinned down at one end on a SiO substrate and an atomic force microscope was used to exert force on the free end while simultaneously recording force and displacement from the equilibrium position [24] (see Figure 3.4). This technique allows a Young's modulus for a multi-walled nanotube to be obtained with no dependence on tube diameter and an average value of 1.28 TPa was obtained.

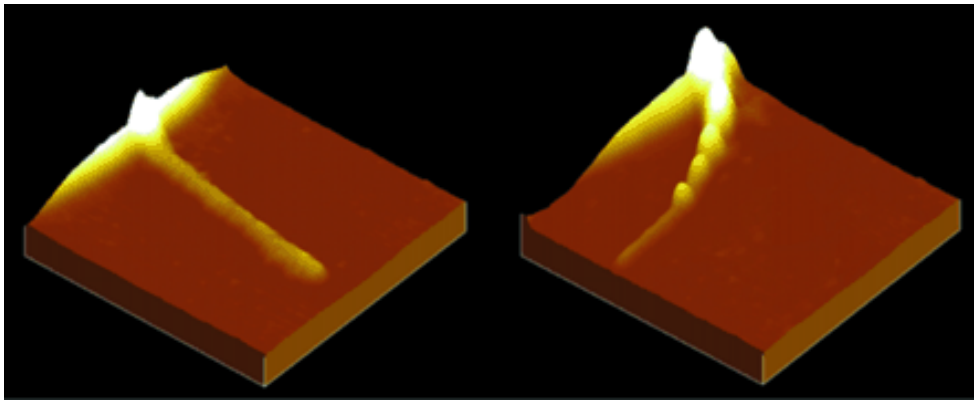

Figure 3.4. The left image shows a 4.4-nm-diameter MWNT pinned at the left side on SiO_2 and in its equilibrium position. The nanotube was then bent by scanning with the AFM tip in contact with the surface. The right image shows bumps along its side which correspond to points at which buckling occurs [24].

3.2. Carbon Nanotube Growth Processes

Carbon nanotubes are synthesized by three primary techniques: carbon arc discharge [25], laser ablation [26], and chemical vapor deposition [27]. A brief description of the history and process of each technique will follow.

3.2.1. Carbon Arc Discharge

The arc discharge method was the first technique used to produce carbon nanotubes, as it was the same method to synthesize fullerene molecules [25]. Krätschmer et al. [25] used this method to produce large quantities (100 mg) of purified C_{60} at a low inert gas pressure in the range of about 100 torr. Graphite electrodes were evaporated at this pressure and the resulting black soot was scrapped from inside the evaporation chamber and dispersed in benzene. C_{60} dissolved in the benzene and the liquid was separated from the soot. Once this liquid was dried it left a residue of the dark crystalline material.

Carbon nanotubes were first produced in large scale quantities by a similar experiment where electric arc discharge occurred between two electrodes under an increased helium or argon gas pressure of about 500 torr [28]. It was found that an increase in the inert gas pressure in the reaction chamber directly increased the yield and purity of the resulting carbon nanotubes (see Figure 3.5). Ebbesen and Ajayan [28] applied a potential of about 18 V between two graphite rods of different lengths. The rods were kept at a constant distance of about 1 mm from each other while the smaller rod was consumed. The high temperature between the two graphite electrodes enabled the sublimation of carbon. Carbonaceous deposits which contained carbon nanotubes formed on the larger rod. The synthesized MWNTs were several microns long and had diameters in the range of 2 – 20 nm [28].

A metal catalyst is needed to grow single-walled carbon nanotubes by carbon arc discharge. Bethune et al. [29] were the first to succeed in producing large quantities of carbon nanotubes by this method. Electrodes were prepared by boring holes in two graphite rods and filling them with fine powdered metals and graphite. They were then vaporized at 95-100 A in a 100-500 torr helium arc fullerene generator. When the cobalt-filled electrode was used, the soot in the chamber was peeled off and characterized under a transmission electron microscope (TEM) at high magnification. Carbon nanotubes with single layer walls and diameters of about 1.2 nm were present [29].

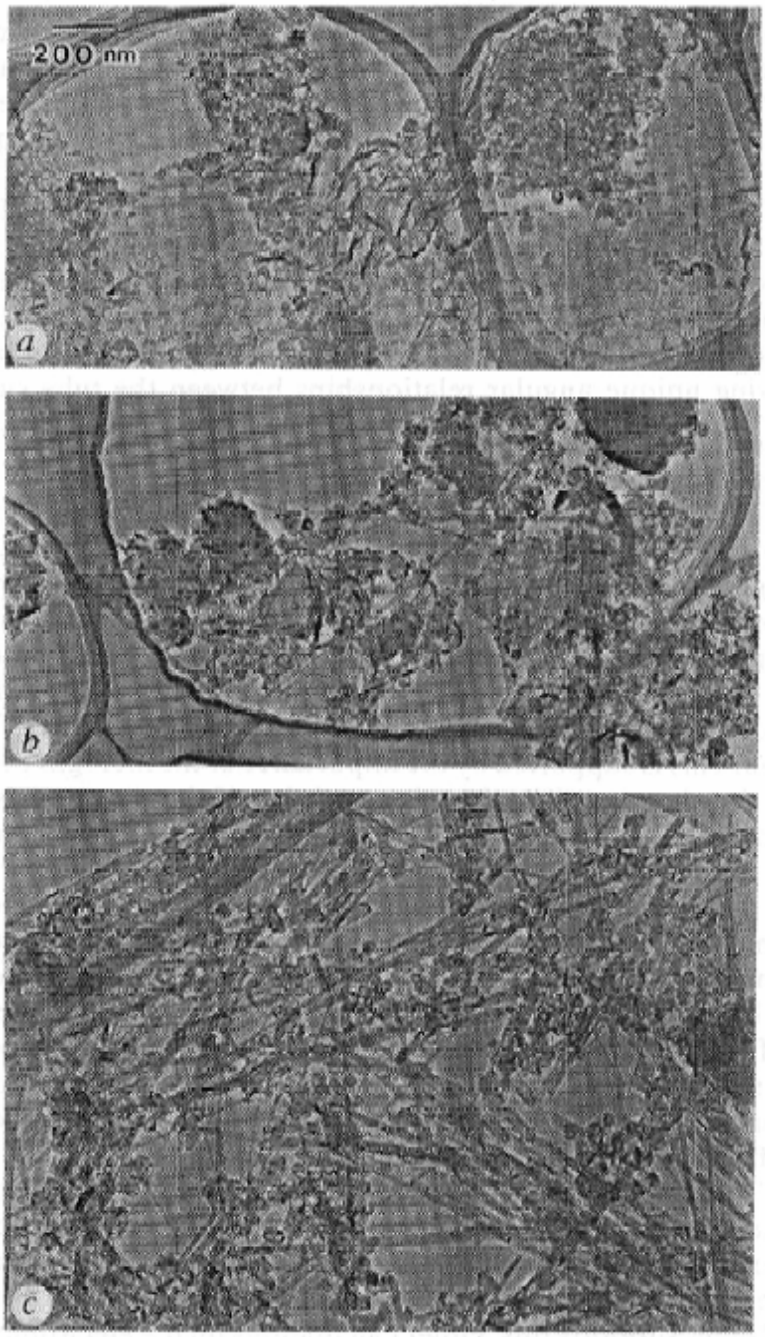

Figure 3.5. Electron micrographs of samples prepared by carbon arc discharge in a helium atmosphere at (a) 20 torr, (b) 100 torr, and (c) 500 torr. There is an increase in number of nanotubes as pressure is increased [28].

3.2.2. Laser Ablation

Laser vaporization had been used for the production of C_{60} molecules (also called buckminsterfullerenes) long before the discovery of the carbon nanotube. In fact, the motivation to produce this form of carbon arises from the theory that it may be an important component of interstellar dust and may be widely distributed in the Universe [30]. Kroto et al. [30] used this technique to first produce fullerene molecules in the gas phase. It involved using a focused pulse laser to vaporize carbon species from the surface of a solid graphite disk into a high density helium flow. Carbon species were vaporized in the helium stream, cooled and partially equilibrated in the expansion, and traveled in the resulting molecular beam to the ionized region. The clusters were then ionized [30].

While performing research on the production of metallofullerenes, Guo et al. [26] found multi-walled carbon nanotubes in the resulting soot from pure carbon target rods (see Figure 3.6). During laser vaporization, a graphite target is placed in the middle of a long quartz tube mounted in a furnace (see Figure 3.7). After the sealed tube has been evacuated, the furnace temperature is increased. The tube is then filled with a flowing inert gas and a scanning laser beam is focused onto the graphite target by way of a circular lens. The laser beam scans across the target surface under computer control to maintain a smooth, uniform face for vaporization. The argon carrier gas flow sweeps most of the carbon species produced by the laser vaporization, high temperature condensation process out of the furnace zone, depositing it as soot on a conical water-cooled copper rod.

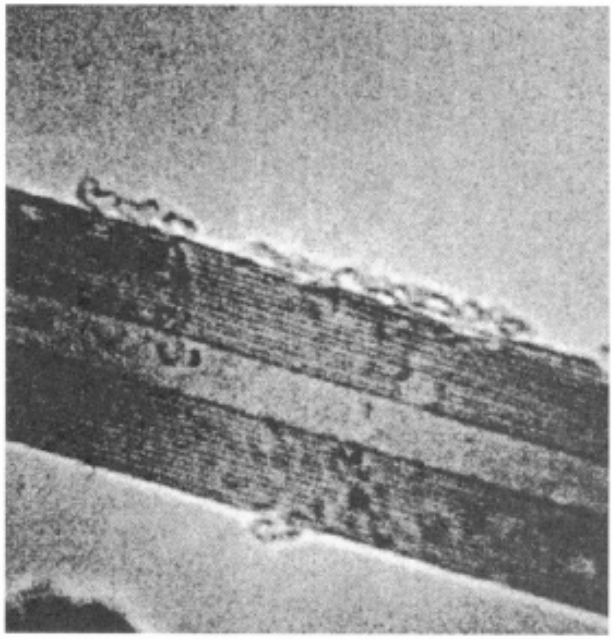

Figure 3.6. TEM image of a MWNT of 2.7 nm inner diameter produced by laser vaporization [26].

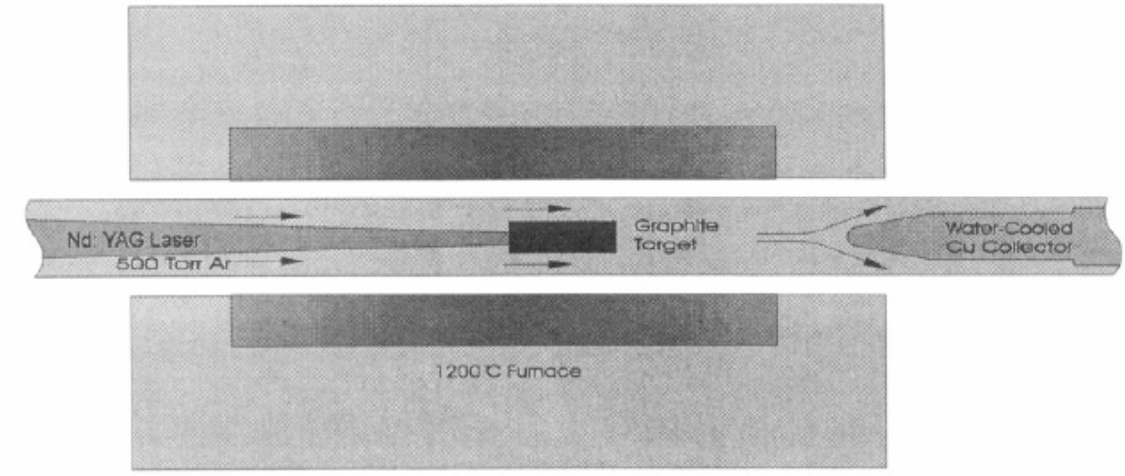

Figure 3.7. Schematic of the laser chamber where carbon nanotubes were first observed [26].

3.2.3. Chemical Vapor Deposition

Carbon nanotube growth via chemical vapor deposition (CVD) involves heating a catalyst to high temperatures in a furnace and flowing a hydrocarbon gas through the tube reactor for a period of time [31] (see Figure 3.8). Materials grown over the catalyst are collected upon cooling the system down to room temperature. Usually, a transition metal such as iron, nickel, or cobalt is used as the catalyst. This is due to the fact that at high temperatures carbon has finite solubility in these metals and the precipitation of carbon from the saturated metal particle leads to the formation of tubular carbon solids [31].

Yudasaka et al. [33] achieved growth of multi-walled carbon nanotubes over a nickel catalyst. Nickel particles were formed by heat-treating various thicknesses of nickel films over a quartz-glass substrate under vacuum. Without breaking vacuum, carbon was deposited over the nickel particles by CVD. The nickel film with a thickness of 5 nm was transformed into nickel droplets by heat treatment. Carbon nanotubes several microns long grew from the nickel droplets by CVD at 700°C (see Figure 3.9).

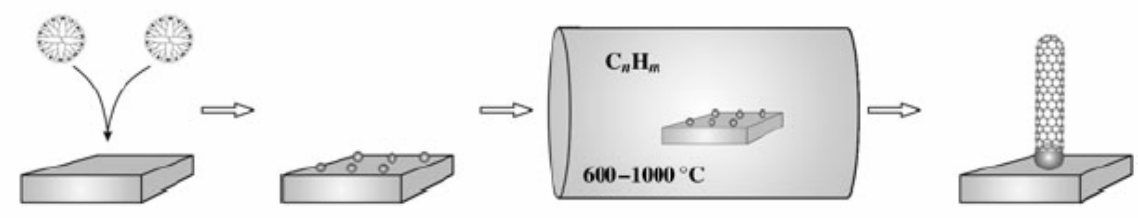

Figure 3.8. Synthesis of individual CNTs by catalyst particles deposited on a substrate [32].

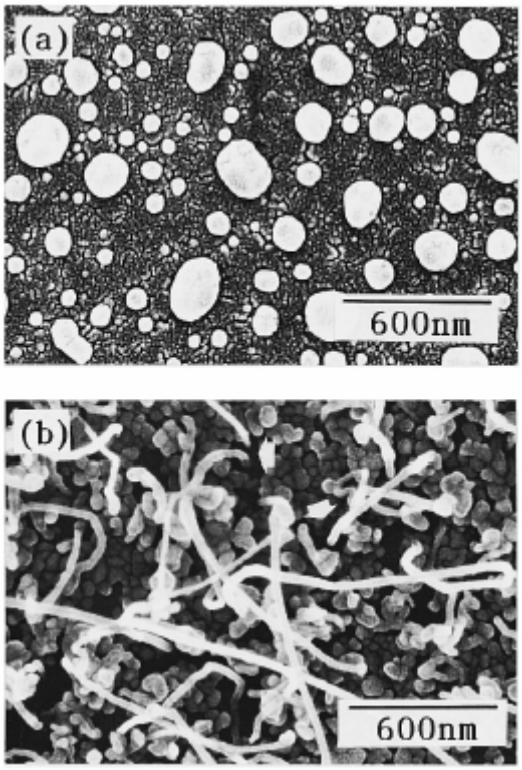

Figure 3.9. Scanning electron micrographs of (a) heat-treated Ni film with thickness of 5 nm and (b) CNT deposit obtained by CVD on Ni droplets appearing in (a) [33].

Chapter Four

Electrode Fabrication Techniques

A typical biosensor consists of the following elements: (1) substrate, (2) receptor, (3) transducer, and (4) signal processor. For the case of the pH and lactate sensors, the substrate is the carbon nanotubes. The receptor is a highly selective sensing element that responds to the substance being measured. It is the functionalized part of the carbon nanotubes. The transducer is a device that converts the physical or chemical changes due to analyte-receptor reactions to another form of physical signal (in general, electronic signals) whose magnitude is proportional to the amount of analyte. The signal processor is the electrochemical analyzer. It is used to filtrate, amplify, and correlate the signal.

4.1. Carbon Nanotube Functionalization

High stability and selectivity of any type of carbon nanotube biosensor is a direct result of the special structure of the nanotube. Altering the structure of a carbon nanotube to make it more stable and specific to one particular analyte is called functionalization.

4.1.1. Chemical Functionalization

Chemical modification of carbon nanotubes is becoming an increasing popular technique in biosensor applications. Chen et al. [34] chemically functionalized SWNTs by an ultrasonic treatment in a solution of nitric and sulfuric acids. From this approach,

the end caps on the tubes opened and holes in the sidewalls were created. The result of this research led to short carbon nanotubes with lengths of 100 to 300 nm with sidewalls modified by many oxygen containing functional groups.

One of the most common forms of oxygen containing functional groups is carboxylic acid in the form of a hydrogen-bonded dimer (see Figure 4.1). This group is predominant at room temperature [35].

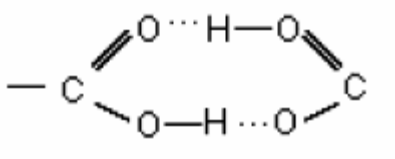

Figure 4.1. Hydrogen-bonded dimer [35].

The oxidatively introduced carboxyl groups represent useful sites for further modification at the sidewalls, as they enable covalent coupling of molecules through the creation of amide and ester bonds (see Figure 4.2) [32]. The presence of this type of functional group allows for the attachment of several other biomolecules, including enzymes.

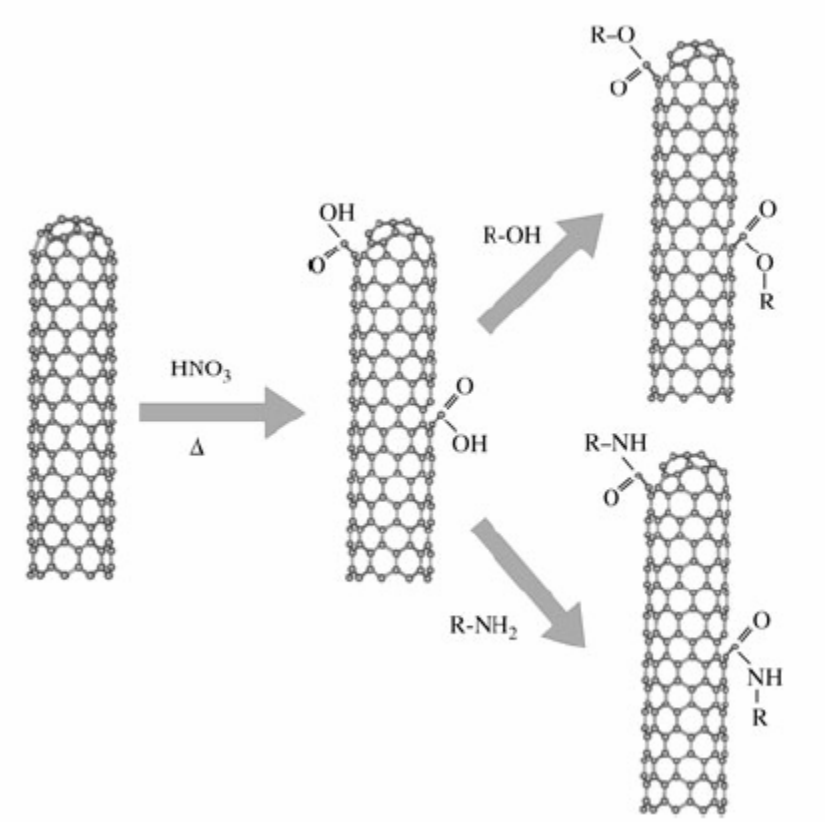

Figure 4.2. Chemical modification of CNTs, followed by subsequent esterification or amidization of the carboxyl group [32].

Chemical functionalization of CNTs has been also been conducted by acidic oxidation, employed to purify low quality nanotube materials [36]. Once purified, the carboxyl groups at the ends of the carbon nanotubes were then converted to the corresponding acid chloride by reaction with $SOCl_2$ at room temperature. Subsequent exposure to NH_2-$(CH_2)_{11}$-SH in toluene at room temperature produced an amide linkage of the nanotube to the alkanethiol. The chemistry was assayed by using the free thiol end to tether the end of the nanotube to a 10-nm diameter gold particle. AFM imaging revealed that most tubes derivatized in this way have a single gold particle bound to at least one of their ends (see Figure 4.3) [36].

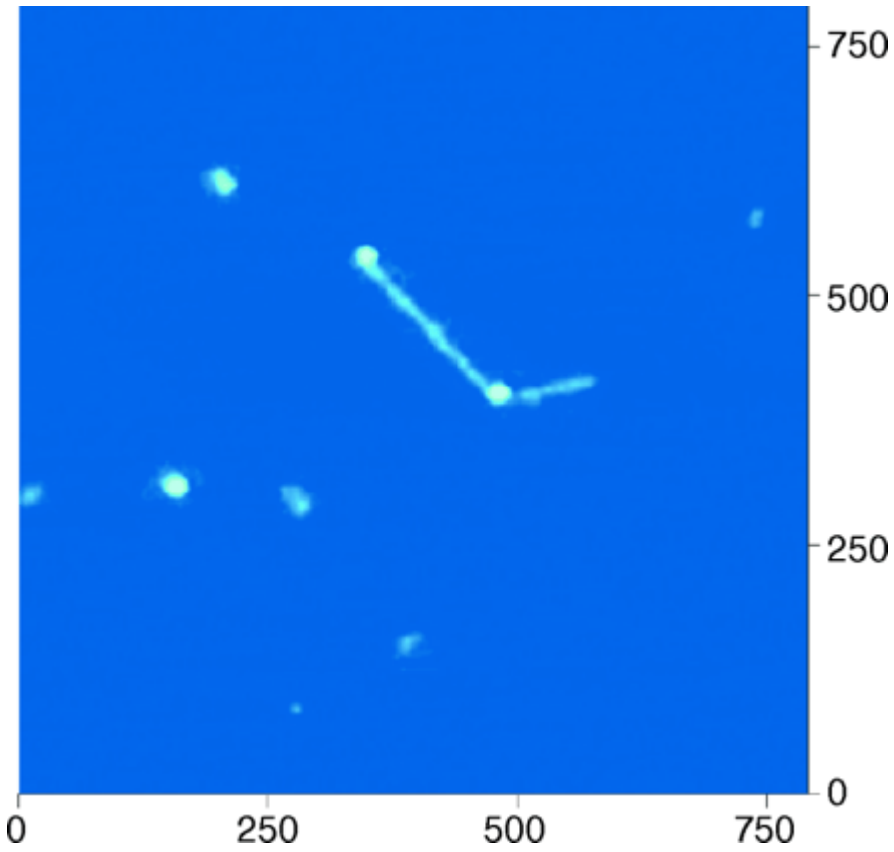

Figure 4.3. Chemical functionalization of CNTs to produce nanotube-to-gold tethers [36].

4.1.2. Electrochemical Functionalization

Another tool to functionalize carbon nanotubes is electrochemistry. In this technique, a constant current or constant voltage is applied to a CNT electrode immersed in a solution that contains a reagent, which results in the generation of a highly reactive species through the electron transfer between the CNT and the reagent [32]. Depending on the reagent used, a polymeric layer is formed on the nanotube. Advantages of electrochemical modification (ECM) include control of film deposition parameters as well as the ability to control surface properties of the nanotube.

Bahr et al. [37] reported the functionalization of small-diameter nanotubes via electrochemical reduction of aryl diazonium salts, in a manner similar to that employed for functionalization of other carbon surfaces. For the derivatization experiments, a piece of bucky paper, formed by filtration of a suspension, was used as the working electrode in a three-electrode cell and immersed in an acetonitrile solution containing the diazonium salt and an electrolyte. The series of diazonium salts used gave differing degrees of functionalization, although a single reason was not clearly responsible for these differences.

Knez et al. [38] reported the reduction of a 4-nitrobenzenediazonium salt was used to attach 4-nitrophenyl groups covalently to single-walled carbon nanotubes deposited on a Si/SiO_2 substrate. The reduction of the 4-nitrobenzenediazonium cation produced a radical species at or near the SWCNT surface (see Figure 4.4). The radical can then attack the tubes, forming a covalent bond to the carbon lattice.

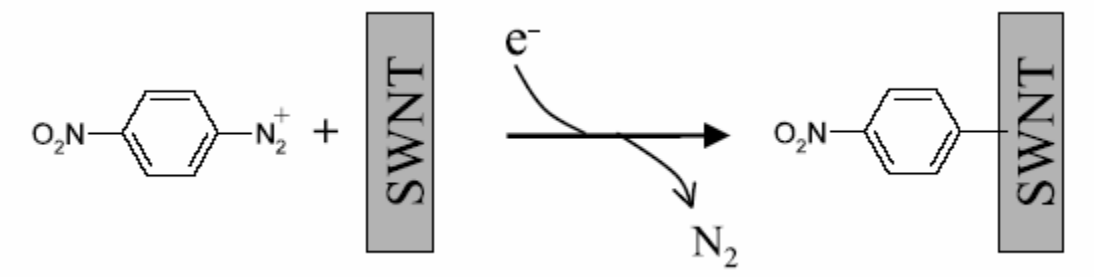

Figure 4.4. Reaction scheme for diazonium salt coupling to functionalize single-wall carbon nanotubes [38].

The degree of modification was found to depend on the concentration of the diazonium salt, the duration of the applied potential, and the magnitude of the applied potential [38].

4.1.3. Functionalization Summary

The following table gives a description of different functionalization methods as well as advantages and disadvantages of each.

Table 4.1. Functionalization Summary

Functionalization Method	*Technique Description*	*Advantages*	*Disadvantages*
Chemical	Ultrasonic acid treatment	CNTs retain their pristine electrical and mechanical properties	Vigorous conditions
Chemical	Free radical addition of alkyl groups terminated with a carboxylic acid	One-step method, nondestructive to sidewall	Long reaction time
Electrochemical	Reduction of aryl diazonium salts	Robust covalent attachment	Varying degree of functionalization

4.2. Immobilization Techniques

During the fabrication of a biosensor, the biological component must be properly attached to the transducer. This process called immobilization. In this context, the physical and chemical stability of the target molecule is usually a necessity. Several other characteristics of a newly modified electrode may be important. For example, the immobilized molecules should remain on the electrode surface when immersed in an electrolyte solution or when the potential of the electrode varies during an electrochemical reaction. Another characteristic is that the immobilized species should remain stable during oxidation and reduction reactions. There are several methods used to immobilize the sensing element, which will be discussed below.

4.2.1. Adsorption

Adsorption is the binding of particles or molecules to a surface. There are two types of adsorption methods: physical and chemical.

4.2.1.1. Physical Adsorption

Physical Adsorption (also called physisorption) is a simple method that requires minimal preparation. Many substances adsorb enzymes on their surface through physisorption. This method tends to be less disruptive to the enzymatic protein than chemical means of attachment because the binding is mainly by hydrogen bonds, multiple salt linkages, and Van der Waals forces. However, the bonding is typically week and suitable for short-term operation. In this respect, the method bears the greatest similarity to the situation found in natural biological membranes and has been used to model such systems. Because of the weak bonds involved, desorption of the protein resulting from changes in temperature, pH, ionic strength or even the mere presence of substrate, is often observed. Another disadvantage is non-specific, further adsorption of other proteins or other substances as the immobilized enzyme is used. This may alter the properties of the immobilized enzyme or, if the substance adsorbed is a substrate for the enzyme, the rate will probably decrease depending on the surface mobility of enzyme and substrate.

4.2.1.2. Chemical Adsorption

Chemical adsorption (also called chemisorption) is a much stronger adsorption technique that involves the formation of covalent bonds. Lane and Hubbard [39, 40] performed extensive electrode modification by chemical adsorption and determined that alkenes adsorb irreversibly on platinum surfaces. For a chemical adsorption reaction to

take place, an electrode surface is exposed in a solution of the adsorbate and then rinsed. If successful, a property such as the cyclic voltammetric redox reaction is observed in a fresh electrolyte solution [41].

4.2.2. Microencapsulation

Microencapsulation involves the encapsulation of the biomolecules within membranes to avoid the loss of the biomolecules and to permit quantities of the substrate to reach the biomolecules. This type of immobilization has several advantages. It is very adaptable, it has close attachment between the biomolecules and the transducer, it limits contamination and degradation, and it is stable towards temperature, pH, ionic strength and composition. Trau and Renneberg [42] developed a scheme of the layer-by-layer process for the encapsulation of microparticular biomaterials, such as microcrystals of catalase or GOX (see Figure 4.5). Encapsulation of glucose oxidase microparticles was achieved by the sequential adsorption of oppositely charged polyelectrolytes onto the GOX biocrystal surface.

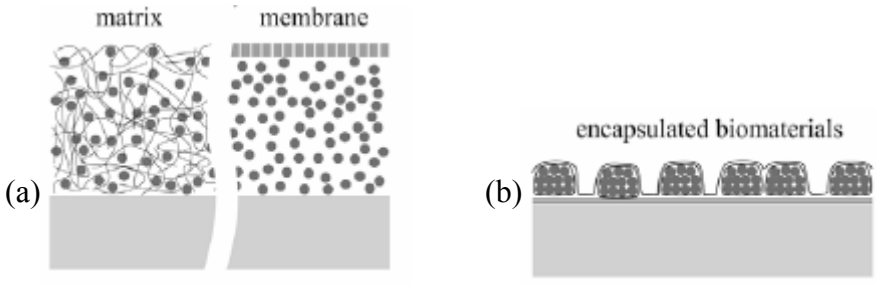

Figure 4.5. (a) Schematic of typical microencapsulation and (b) Schematic based on layer-by-layer encapsulation [42].

4.2.3. Entrapment

Entrapment is the process by which a biomolecule is trapped inside a polymer. The biomolecule is mixed with a monomer solution, which is then polymerized to a gel, trapping the biomaterial inside. The most common polymer used for this method is polyacrylamide. In order for the entrapment to work well, several issues should be achieved. Firstly, a high percentage of the enzymes must be initially retained in gel matrices. Secondly, the enzyme activity must be preserved. And thirdly, the enzymes must be physically restrained from diffusing back into the substrate solution at a later time. Some disadvantages of immobilization via entrapment are the loss of enzymatic activity due to the polymerization process and the large response time for the sensor as the reactants diffuse through the polymer.

Vidal et al. [43] developed a cholesterol amperometric biosensor using entrapment as the immobilization technique. Several configurations of polymer film thickness were designed for study and comparison of their performance. The influence of polypyrrole (PPy) film thickness on the cholesterol biosensor response is very important because it determines the enzyme loading, and hence the sensitivity of the biosensor, its selectivity, and the time of response. The highest sensitivity for the Pt/PPy–cholesterol oxidase (COX) biosensor was obtained at a film thickness corresponding to an overall electropolymerization charge of 10 mC cm^{-2} (about 25 nm thickness).

4.2.4. Cross-Linking

Cross-linking involves chemically bonding a biomaterial to solid supports or to another material such as a gel. Cross-linking is usually best used in conjunction with one

of the other immobilization methods. It is used mostly as a means of stabilizing adsorbed enzymes and for preventing leakage from polyacrylamide gels. The most common reagent used for cross-linking is glutaraldehyde. Cross-linking reactions are carried out under relatively severe conditions. These harsh conditions can change the conformation of active center of the enzyme; and so may lead to significant loss of activity. Other disadvantages include limitation of diffusion of the substrate and poor mechanical strength and rigidity of the electrode material.

Xu et al. [44] demonstrated that thionine and horseradish peroxide (HRP) were successfully co-immobilized by their cross-linking with glutaraldehyde (GA) on a glassy carbon electrode. To immobilize HRP and thionine by cross-linking method, 5 μL of 10 mg/mL HRP and 1 mol L^{-1} thionine in pH 6.9 phosphate buffer solution containing 10 % glutaraldehyde and 5.0 % (w/v) bovine serum albumin (BSA), which linked with glutaraldehyde and formed a stable matrix on the electrode surface, was applied to the electrode surfaces, allowed to air dry for 3 h, and rinsed thoroughly with the buffer. The enzyme electrode exhibited high efficiency of bioelectrocatalytic reduction of hydrogen peroxide via thionine and also possessed good stability and reproducibility for long-term use.

4.2.5. Covalent Bonding

A covalent bond is a bond between two atoms, in which they share a pair of electrons. Covalent bonding is used as an immobilization technique when the bond occurs between a functional group in the biomaterial and the support matrix. Reactions must be performed at low pH and mild temperatures for covalent bonding. An advantage

of covalent bonding is that the enzyme is permanently attached to the support material; this enables good electrical contact. However, this type of bond will decrease the enzyme activity and will also decrease the sensitivity of the electrode during its shelf life.

Rahman et al. [45] fabricated amperometric choline biosensors by the covalent immobilization of the enzyme choline oxidase (ChO) and the bi-enzyme of ChO/horseradish peroxidase (ChO/HRP) onto poly-5,2′:5′,2″-terthiophene-3′-carboxylic acid (poly-TTCA) modified electrodes (CPMEs). CPME was immersed in a 0.1 M phosphate buffer solution (pH 7.0) containing 10.0 mM EDC for 6 h to activate the carboxylic groups of the poly-TTCA film. Then, CPME treated with EDC was washed with a buffer solution and subsequently incubated in 0.1 mg ml^{-1} of ChO in a 0.1 M phosphate buffer (pH 8.0) solution for 12 h at 4 °C. By this step, ChO was immobilized on the poly-TTCA film through the formation of covalent bond between carboxylic acid groups of the polymer and amine groups of the enzyme.

Chapter Five

Experimental

5.1. Carbon Nanotube Functionalization

5.1.1. Carboxylic Acid Functionalization

All carbon nanotubes used in the electrode fabrications were single-walled, purchased from Sigma-Aldrich, and functionalized in the laboratory. The SWNTs were chemically functionalized by a previously described technique [46]. Purified SWNTs were placed in a 250-mL flask filled with 50 mL of dry o-dichlorobenzene and sonicated for 30 min. to obtain a SWNT suspension solution. The latter was heated at 80-90 °C for 10 days while each day 0.5 g of peroxide was added. After the reaction was complete, the suspension was cooled and poured into a 500-mL Erlenmeyer flask containing a large amount of tetrahydrofuran and sonicated for 15 min. The obtained solution was filtered using a 0.2-μm pore size polytetraflouroethylene (PTFE) membrane. Functionalized SWNTs were collected on the membrane, then placed in 100 mL of ethanol, sonicated for 20 min., and then filtered again. During the filtration, a large amount of ethanol was repeatedly used to completely wash off the unreacted peroxides and the reaction byproducts.

5.1.2. Lactate Oxidase Functionalization

For the construction of the lactate sensor, the previously functionalized carbon nanotubes were further modified to be sensitive only to lactate. 1 mL of SWNT-COOH was placed in a 10-mL beaker and dried in an oven overnight at 30°C. The carbon nanotubes were then rinsed with 1 mL of deionized water and again dried overnight at 30°C. From the dried batch of nanotubes, 6.5 mg of CNTs were weighed and placed in a separate test tube with 75 µL deionized water and shaken for 5 min.

Lactate oxidase (LOX) was purchased from Sigma-Aldrich. One international unit (IU) is the amount of enzyme that catalyses the conversion of one micromole of substrate per minute. 10 IU of LOX were added to the CNTs suspended in 75 µL of deionized water. This tube was then shaken for 3 hr. to ensure adequate functionalization.

5.2. Electrode Preparation

5.2.1. pH Electrode

A polished 3 mm-diameter glassy carbon electrode was prepared firstly with 1.0 µm alpha alumina powder and secondly with 0.3 µm alpha alumina powder. The pH electrode was prepared by the following method. 5 µL of SWNTs functionalized with the carboxylic acid group were added to 200 µL of deionized water. The solution was then shaken for 5 min. to ensure uniform suspension of the SWNTs in the water. From this solution, 5 µL was pipetted onto the surface of the polished glassy carbon electrode and immobilized via physical adsorption. This modified glassy carbon electrode with SWNT-COOH was then placed in an oven overnight at 30°C to dry.

5.2.2. Lactate Electrodes

Several different fabrication techniques were tested for the lactate sensor. Two methods are described.

5.2.2.1. CNTs on Thin Film Substrate

Indium tin oxide (ITO) was sputtered onto a 2-in. diameter silicon substrate to a thickness of 400 Å. From this wafer, several 1.5-cm × 0.5-cm pieces were cut. Initially, 10 µL of functionalized CNTs with LOX were dropped onto the small electrodes and dried at room temperature overnight. However, once placed in the phosphate buffer solution containing lactate the CNTs would lose adhesion to the ITO and almost immediately begin to fall off from the chip and into the solution. To remedy this pitfall, colloidal silver paint was purchased from Ted Pella.

For the second attempt, the silver paint was used to bond the carbon nanotubes to the Si/ITO substrate. A thin layer of paint was brushed on top of the ITO and then 10 µL of CNT-COOH-LOX was dropped onto the paint (see Figure 5.1). This modified electrode was allowed to dry at room temperature overnight.

It was calculated that in 10 µL of solution there are 0.8667 mg of functionalized carbon nanotubes. The approximate dimensions of a single nanotube are 1.5-nm diameter × 20-µm length. The density of a CNT was found to be 2.1 g/cm^3. From these values, it was calculated that one CNT weighs approximately 9.89602×10^{-17} g. So, in 0.8667 mg of CNTs, there are about 8.75773×10^{12} carbon nanotubes.

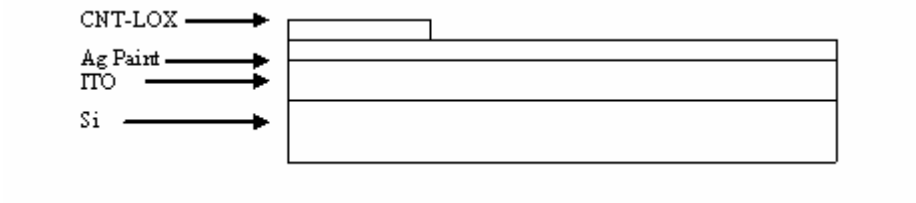

Figure 5.1. Schematic drawing of CNT-LOX on Si/ITO electrode.

5.2.2.2. CNTs on Glassy Carbon

The fabrication of the lactate sensor on glassy carbon is similar to that of the pH sensor. 5 µL of CNT-COOH-LOX were dropped onto a 3-mm diameter glassy carbon electrode. There are 0.4333 mg of the functionalized carbon nanotubes in the 5 µL solution. This amount equates to about 4.37886×10^{12} carbon nanotubes. The modified electrode was then allowed to dry at room temperature overnight.

5.3. Characterization

The carboxylic acid functionalized carbon nanotubes were characterized by Fourier infrared spectroscopy (FTIR) as well as by electrochemical analysis. The lactate oxidase functionalized carbon nanotubes were characterized by the previous methods as well as by scanning electron microscopy (SEM).

5.3.1. Fourier Transform Infrared Spectroscopy (FTIR)

A wavenumber, expressed in cm^{-1}, is the radiation in the vibrational infrared region of the electromagnetic spectrum [47]. Wavenumbers are the reciprocal of wavelengths and can be converted to frequency by multiplying it by the speed of light. The vibrational infrared wavenumber range is from 4000 to 400 cm^{-1}.

When infrared radiation is applied to a material, molecules are excited to a higher energy state and absorb only selected frequencies. The frequencies of infrared radiation which match the natural vibration frequencies of a particular molecule that are absorbed along with the absorbed energy increases the amplitude of the vibrational motions of the bonds of the molecule [47]. Every type of bond has a different natural frequency of vibration; thus, no two molecules of a different structure have the exact same infrared absorption pattern, or infrared spectrum. In this way, FTIR proves to be a useful means to examine the bonds of the carboxyl functional groups as well as lactate oxidase to the carbon nanotubes (see Figure 5.2).

Carboxylic acids show a strong band for the C=O bond at 1610 cm^{-1}. The O–H stretch band appears very broadly from 3400 – 2400 cm^{-1} [47]. For the CNT-COOH, it centers on 2879 cm^{-1}.

Lactate oxidase can be identified through the absorption of the amine groups. N–H bend in primary amines occurs in the broad range of 1640 – 1560 cm^{-1} and for the functionalized CNTs with LOX it centered on 1558 cm^{-1}. N–H out-of-plane bending absorption is typically observed near 800 cm^{-1}. C–N stretch occurs in the range of 1350 – 1000 cm^{-1} [47]. For the CNT-LOX, N–H out-of-plane bending was observed at 798 cm^{-1} and C–H stretch was observed at 1190 cm^{-1}.

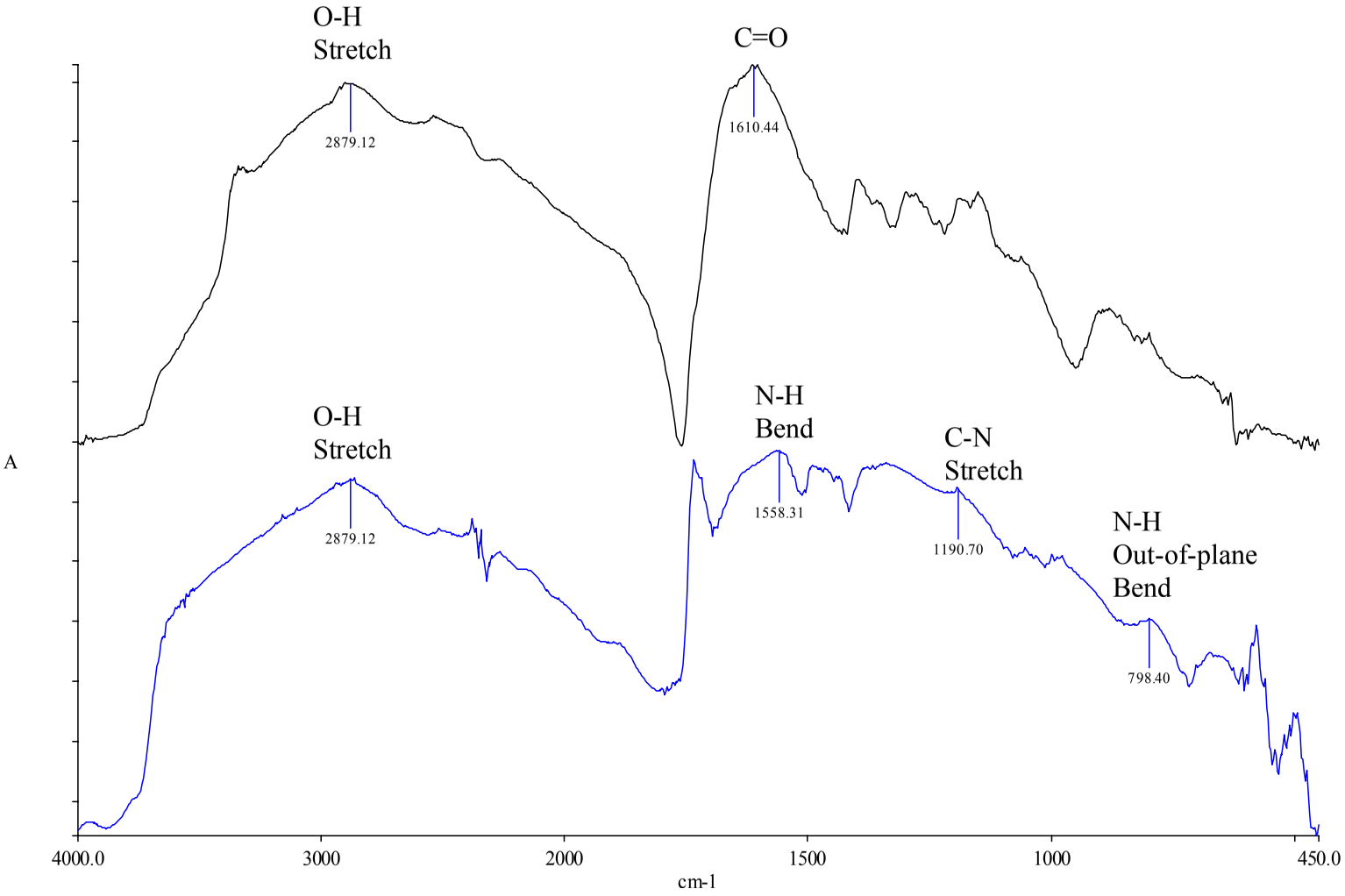

Figure 5.2. Comparison of CNT-COOH (top) and CNT-COOH-LOX (bottom).

5.3.2. Scanning Electron Microscopy (SEM)

The scanning electron microscope can be used to image surface features of a sample at 10 to 100000 ×. Depending on the sample, it can provide resolution in the nanometer range. The SEM works very similar to that of a television. The electron gun produces a stream of monochromatic electrons. The stream is condensed by the first condenser lens. This lens is used to both form the beam and limit the amount of current in the beam. The beam is then constricted by the condenser aperture, eliminating some high-angle electrons. The second condenser lens forms the electrons into a thin, tight, coherent beam. A set of coils then scans the beam in a grid. The objective lens focuses the scanning beam onto the part of the specimen desired. When the beam strikes the sample interactions occur inside the sample and are detected. Before the beam moves to its next dwell point these instruments count the number of e^- interactions and display a pixel on a CRT.

The electrode prepared by dropping LOX-modified CNTs onto the silver painted Si/ITO substrate was examined by a scanning electron microscope (see Figures 5.3-5.8). The following images verify the porosity of the silver paint as well as the alignment of the carbon nanotubes in the paint. The CNTs are aligned randomly, with some embedded in the silver paint more than others. Certain CNTs are suspended in the paint only by their ends. Also, some CNTs have only one end anchored in the paint with the rest of the nanotube completely exposed to the lactate solution.

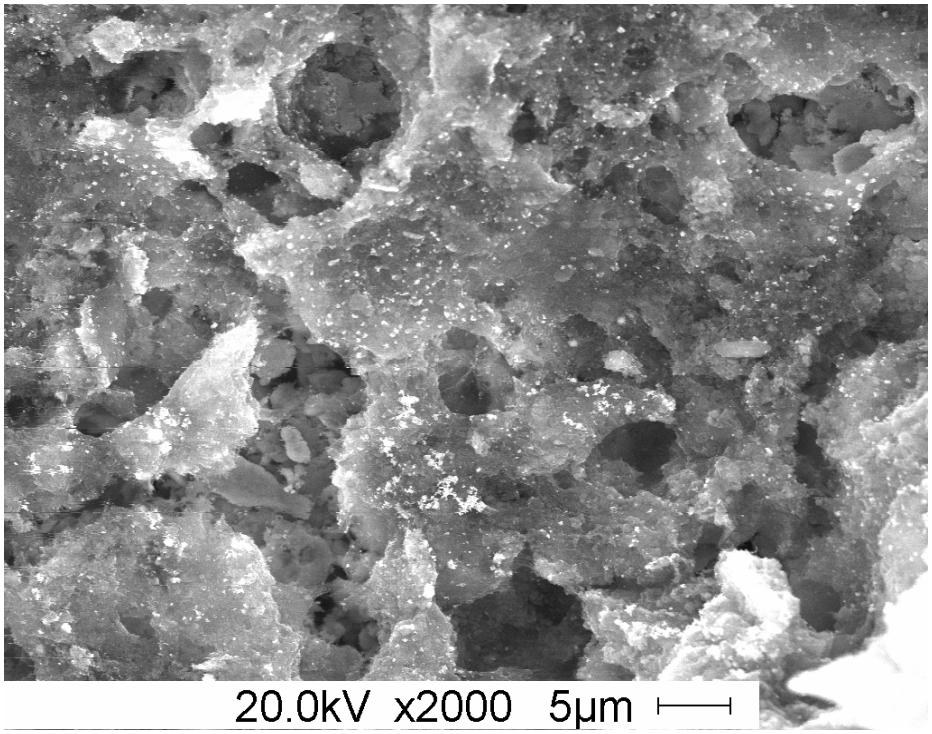

Figure 5.3. Silver paint on Si/ITO.

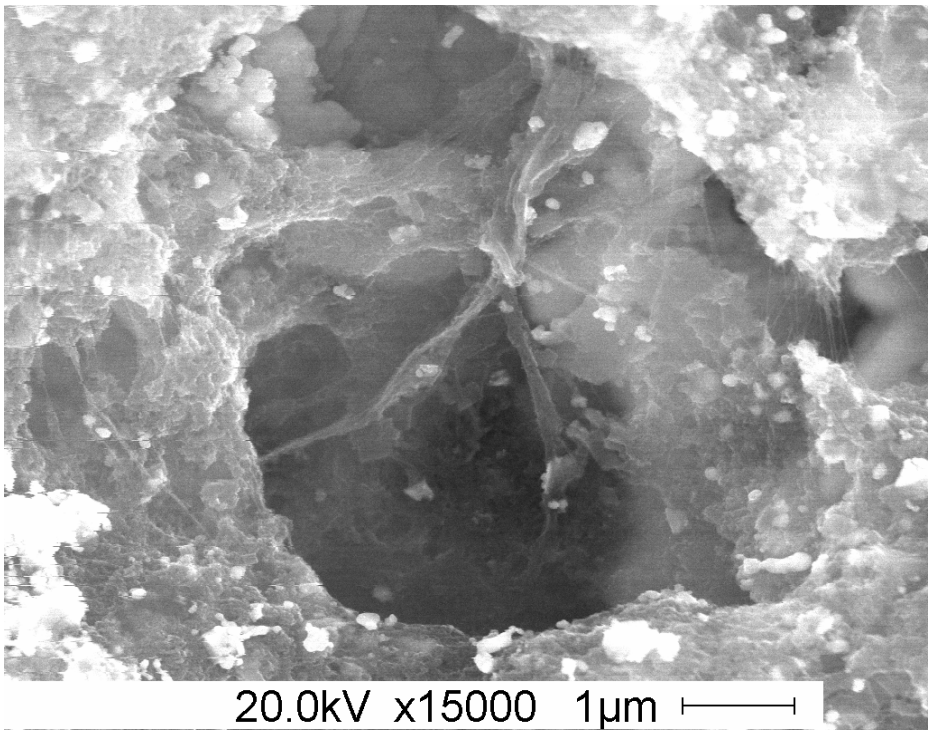

Figure 5.4. Silver paint at higher magnification.

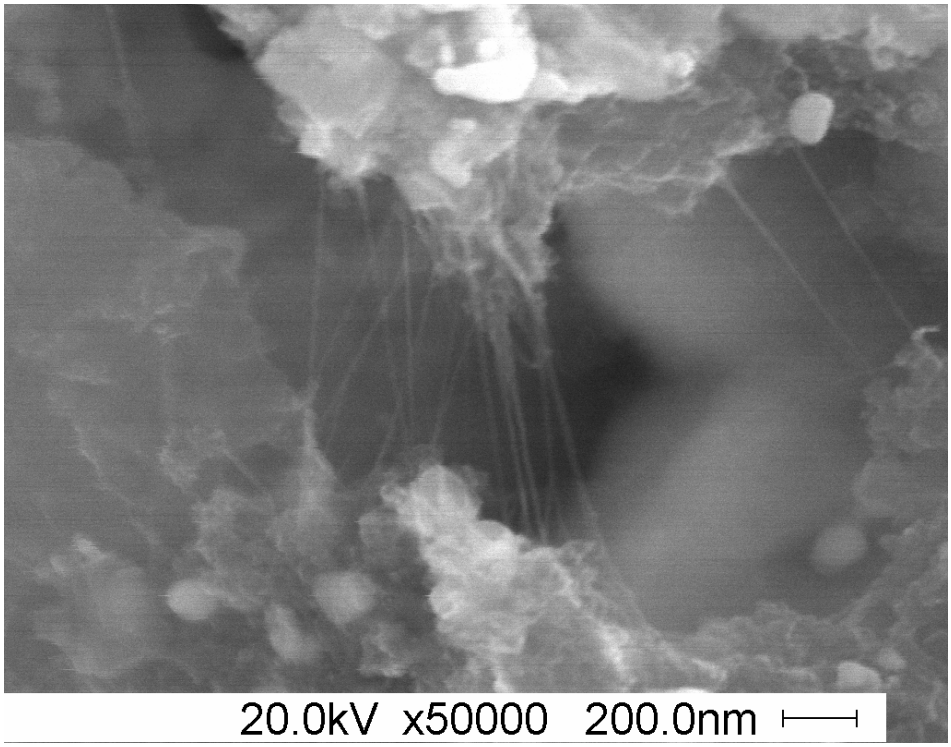

Figure 5.5. Carbon nanotubes suspended in silver paint on lactate electrode.

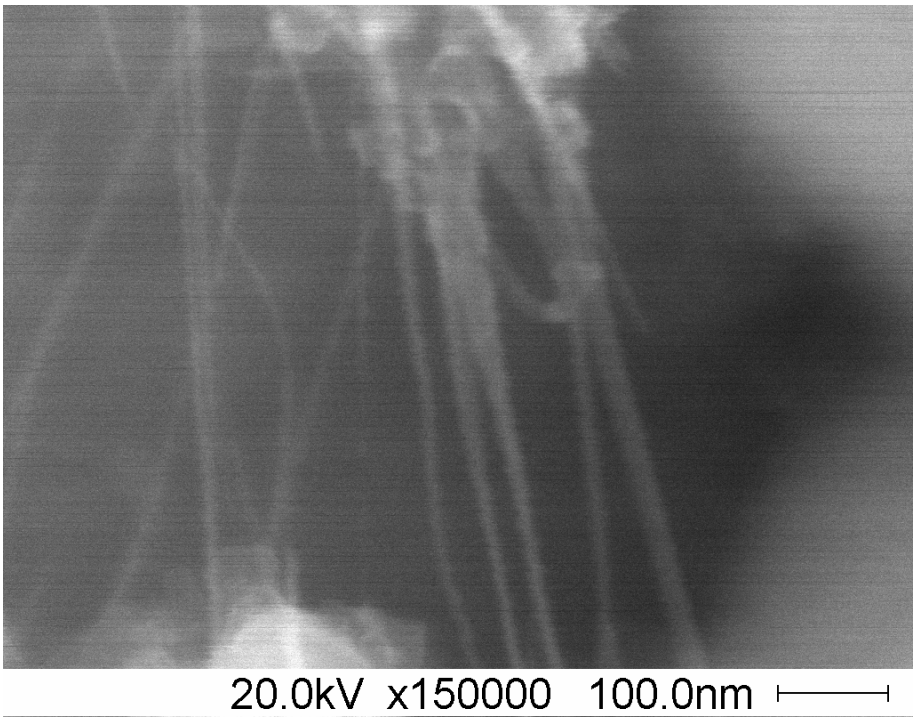

Figure 5.6. Carbon nanotubes at higher magnification.

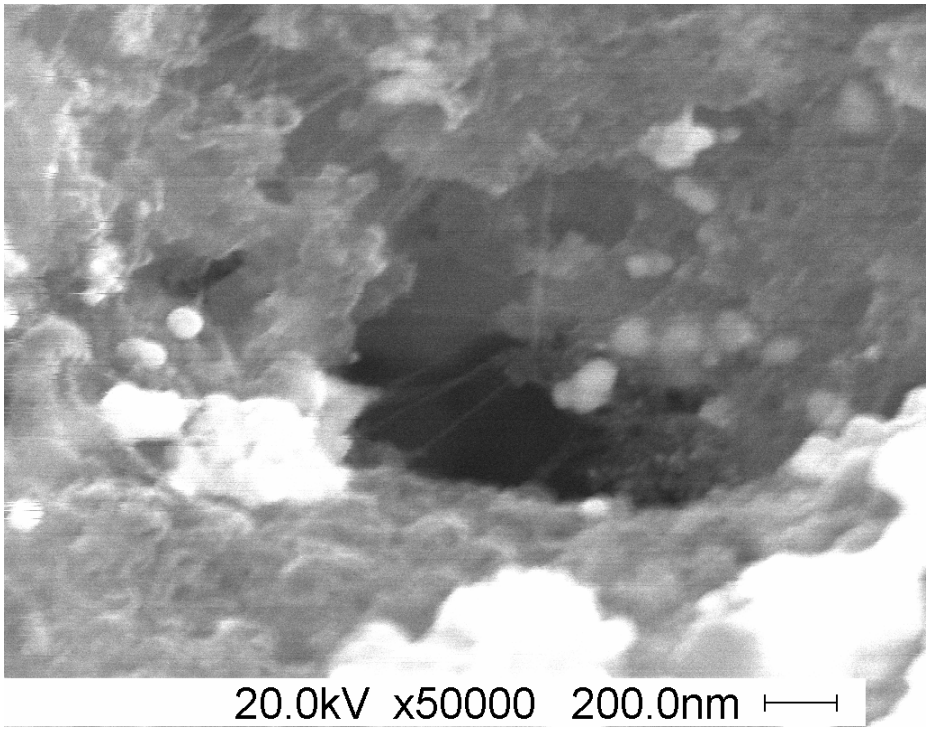

Figure 5.7. Random orientation of CNTs spread throughout the silver paint.

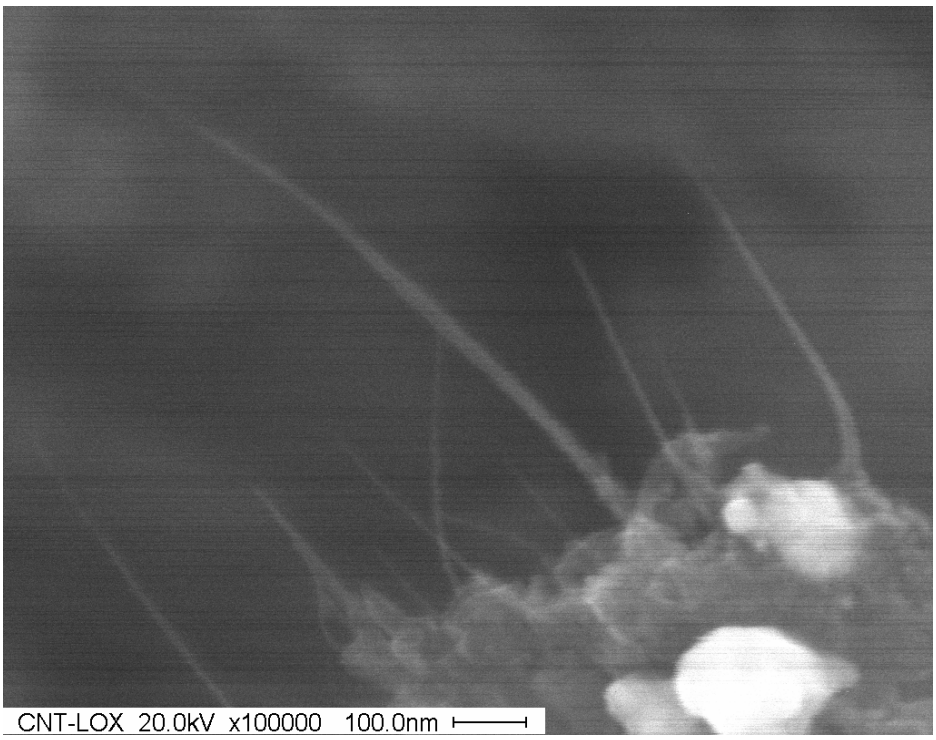

Figure 5.8. Carbon nanotubes with one end anchored in silver paint.

5.3.3. Electrochemical Characterization

Different electrochemical techniques can be used for biosensing applications (depending on the nature of the analyte, the character of the sample matrix, and sensitivity or selectivity requirements). Most of these techniques fall into two major categories: amperometric and potentiometric characterization.

5.3.3.1. Amperometry

Amperometric sensors are based on the detection of electroactive species involved in the chemical or biological recognition process. The signal transduction process is accomplished by controlling the potential of the working electrode at a fixed value (relative to a reference electrode) and monitoring the current as a function of time. The applied potential serves as the driving force for the electron transfer reaction of the electroactive species. The resulting current is a direct measure of the rate of the electron transfer reaction. It is thus reflecting the rate of the recognition event, and is proportional to the concentration of the target analyte.

5.3.3.2. Potentiometry

In potentiometric sensors, the analytical information is obtained by converting the recognition process into a potential signal, which is proportional, in a logarithmic fashion, to the concentration of a species generated or consumed in the recognition event. Such devices rely on the use of ion selective electrodes for obtaining the potential signal. A perm selective-ion-conductive membrane (placed at the tip of the electrode) is designed to yield a potential signal that is primarily due to the target ion. Such response is measured under conditions of essentially zero current.

Voltammetry is the study of the current-voltage relationships observed when electroactive species in solution are subject to oxidation or reduction at electrodes under carefully controlled conditions [48]. One type of voltammetry is cyclic voltammetry. A cyclic voltammogram consists of plotting current that flows as a function of the applied potential. The amount of current that flows is directly related to the amount of species present (see Figure 5.9).

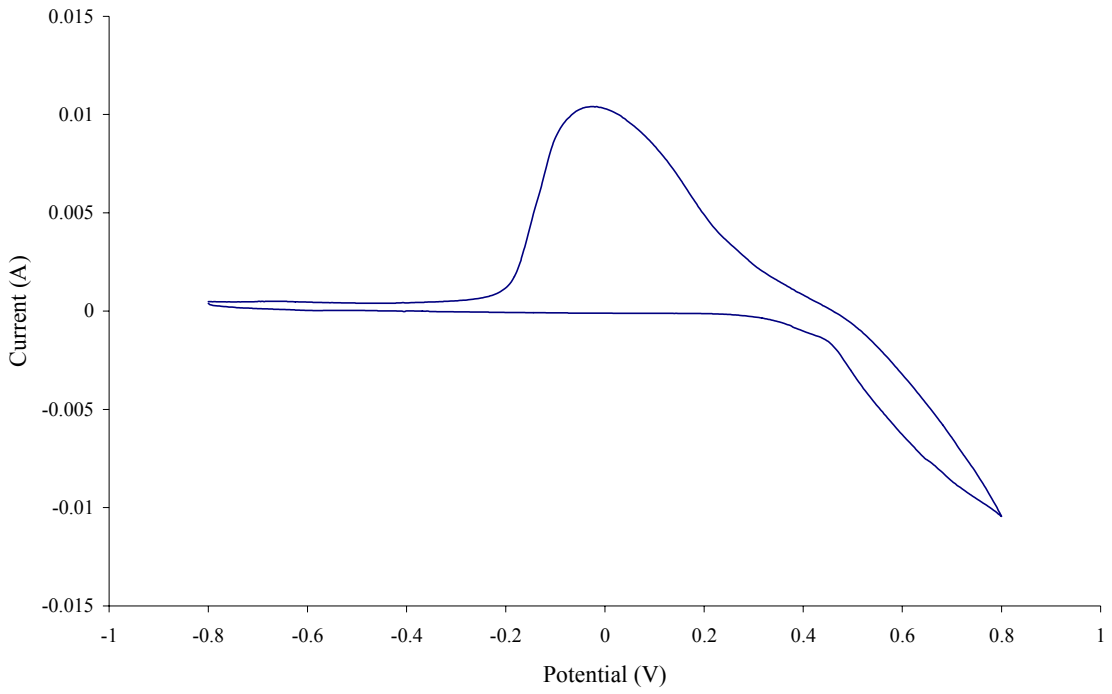

Figure 5.9. Cyclic voltammogram of CNT-LOX at 0.05 M lactate.

Although cyclic voltammetry is a very useful quantitative technique, it cannot be used to detect every biological and chemical species. There exist several voltammetry templates other than cyclic, such as linear or square wave.

Chapter Six

Results and Discussion

6.1. pH Sensor

Three types of voltammetry techniques were tried to achieve high pH sensitivity: cyclic, linear, and square wave. Square wave voltammetry provided to be the most sensitive technique to changes in pH with the functionalized CNT-COOH electrode. In square wave voltammetry a square wave potential superimposed to a staircase potential is applied to the electrode (see Figure 6.1). Using square wave voltammetry, an applied voltage was swept across the CNT electrode and pH was detected during association of the H^+ ions to the COO^- group.

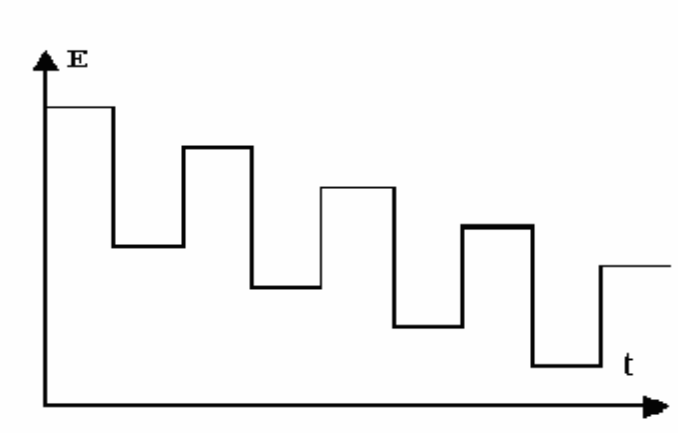

Figure 6.1. The square wave curve, showing potential as a function of time.

All pH sensing was carried out in a standard three electrode electrochemical cell at room temperature. The cell contained 10 mL of 0.1 M K_2HPO_4 and 0.1 M KH_2PO_4 buffer solution. A solution of 50 % HCl or a solution of 0.1 M NaCl was used to adjust the pH of the phosphate buffer. The electrodes in the cell were as follows:

1. Working Electrode: Functionalized carbon nanotubes with carboxylic acid groups. It provides the surface for electron transfer to occur.
2. Reference Electrode: Ag/AgCl (saturated KCl). The potential is applied between the working and reference electrodes.
3. Counter Electrode: Platinum wire. The current flow is measured between the working and counter electrodes.

The potential scan rate for all experimental runs was 0.1000 mV s^{-1} and the step height was 2.0000 mV. The scan rate is important because it must be a compromise between adequate resolution and required time for analysis. A high scan rate will be too coarse for adequate resolution and a slower scan rate will give better resolution but at a longer analysis time.

All of the buffer solutions were tested with a Corning Scholar 425 pH meter to verify the accuracy of the carbon nanotube based pH electrode. The CNT-COOH sensor exhibited extremely high accuracy with only about 1.22 % error. A linear response was observed for pH 1-10 (see Figures 6.2 – 6.4). For each increase in pH, the electrode experiences a negative shift in potential. The calibration line was created by taking the voltage values at the peaks of each curve and plotting this voltage value by its respective pH value. Note that the inconsistent vertical spacing of the current between the peak values does not affect the results. Only the horizontal shifts relating to voltage are

considered. By the definition of voltammetry, for this senor the change in potential is proportional to the change in hydrogen ion concentration and the current reading is not necessary for this technique. For example, a solution with a pH 7 is neutral because it has the same amount of H^+ ions and OH^- ions. So, a voltammetric response for pH 7 should be at a zero potential and any decrease in H^+ ions will result in a negative potential.

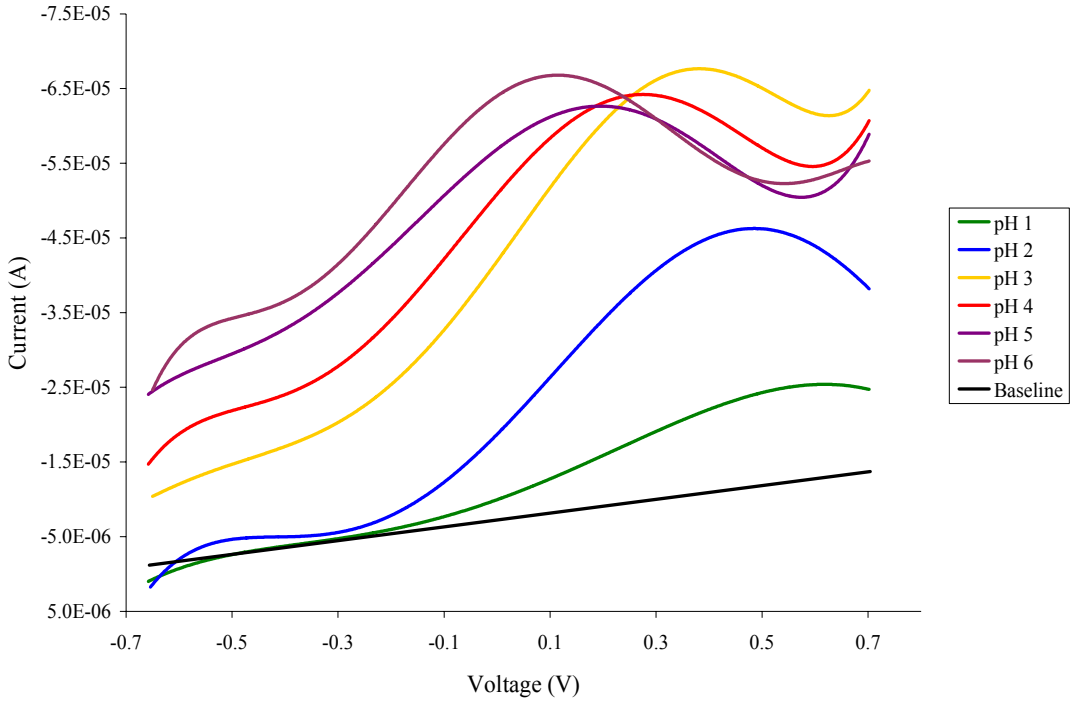

Figure 6.2. CNT-COOH pH electrode results for pH 1-6.

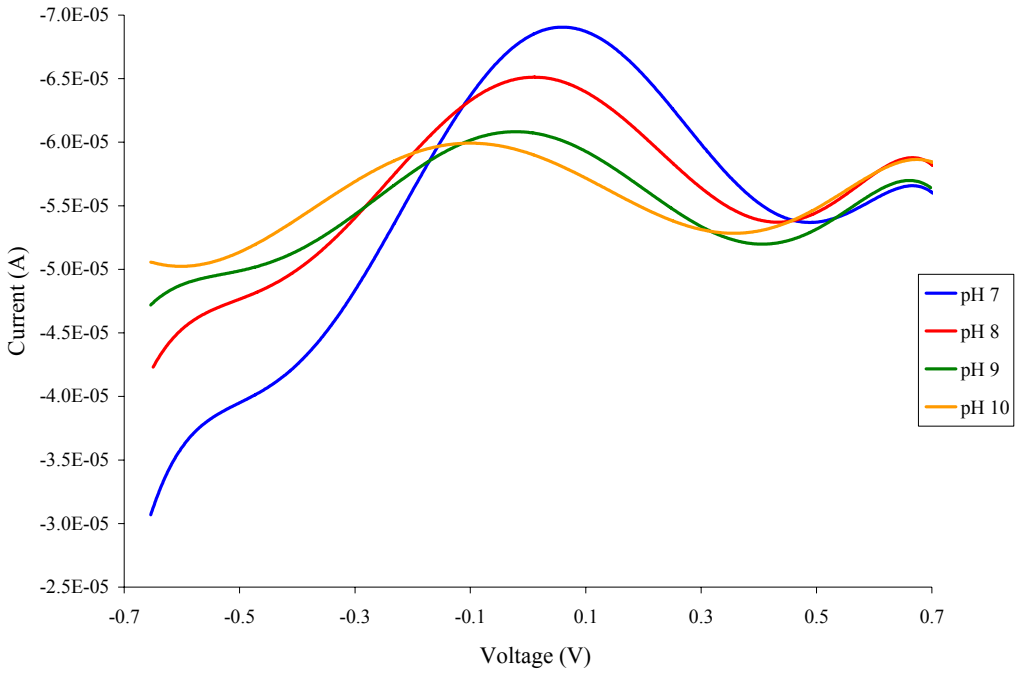

Figure 6.3. CNT-COOH pH electrode results for pH 7-10.

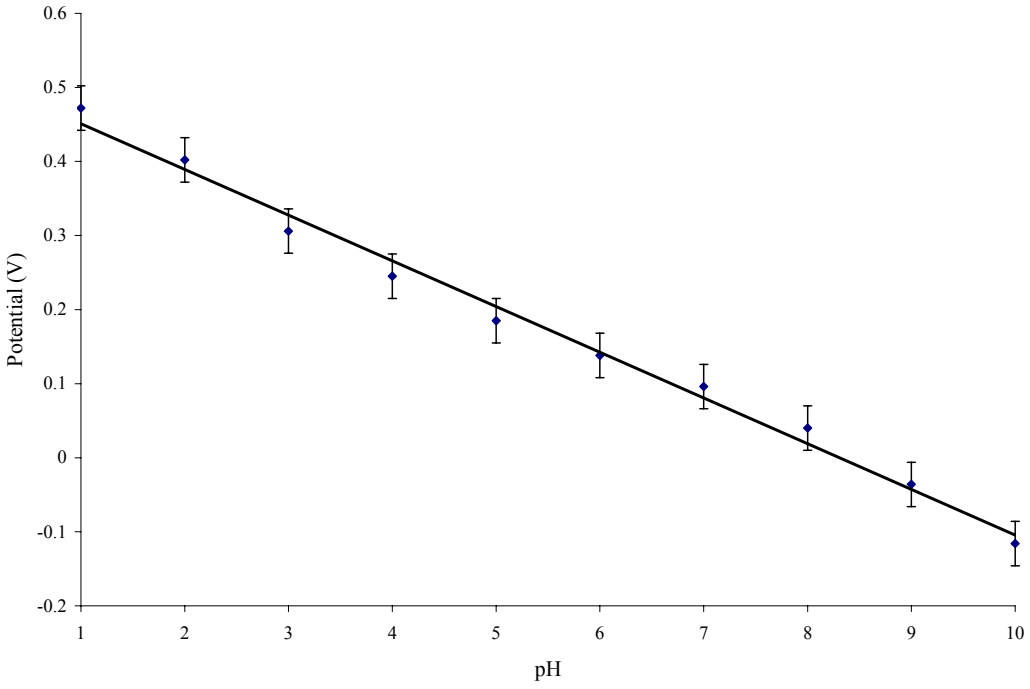

Figure 6.4. CNT-COOH linear calibration line.

6.2. Lactate Sensor

6.2.1. Functionalized CNTs on Si/ITO

All experimental runs were carried out in a 10 mL electrochemical cell containing 0.1 M K_2HPO_4 and 0.1 M KH_2PO_4 buffer solution and varying concentrations of lactic acid at room temperature. The reference and counter electrodes were the same as in the pH sensor experiments. The following electrochemical reaction occurs at the CNT-LOX electrodes:

$$\text{Lactate} + O_2 \xrightarrow{LOX} \text{Pyruvate} + H_2O_2$$

Furthermore, hydrogen peroxide is oxidized as follows:

$$H_2O_2 \rightarrow O_2 + 2H^+ + 2\ e^-\text{'s}$$

The sensor works by measuring how many electrons are transferred to the working electrode. In this case, for every two transferred electrons to the working electrode, one molecule of lactate is detected.

This sensor worked in the range of 0.01 M – 0.05 M lactic acid (see Figure 6.5). The calibration line was calculated by taking the peak current reading for each concentration and subsequently plotting current versus concentration (see Figure 6.6). However, by continually increasing the amount of lactic acid in the electrochemical cell, the silver paint lost adhesion to the ITO thin film and the silver paint with the immobilized carbon nanotubes peeled off the of Si/ITO substrate. Upon examination by SEM, the silver paint was observed to be extremely porous (see Section 5.3.2). It is important to note that failure occurred at higher lactate concentrations due to loss of contact between the LOX functionalized carbon nanotubes and the ITO thin film via the silver paint. The peaks are not as well defined as they could be due to the silver paint

interfering and reacting in the electrochemical cell. This phenomenon also caused the peaks to not be vertically linearly spaced with respect to current.

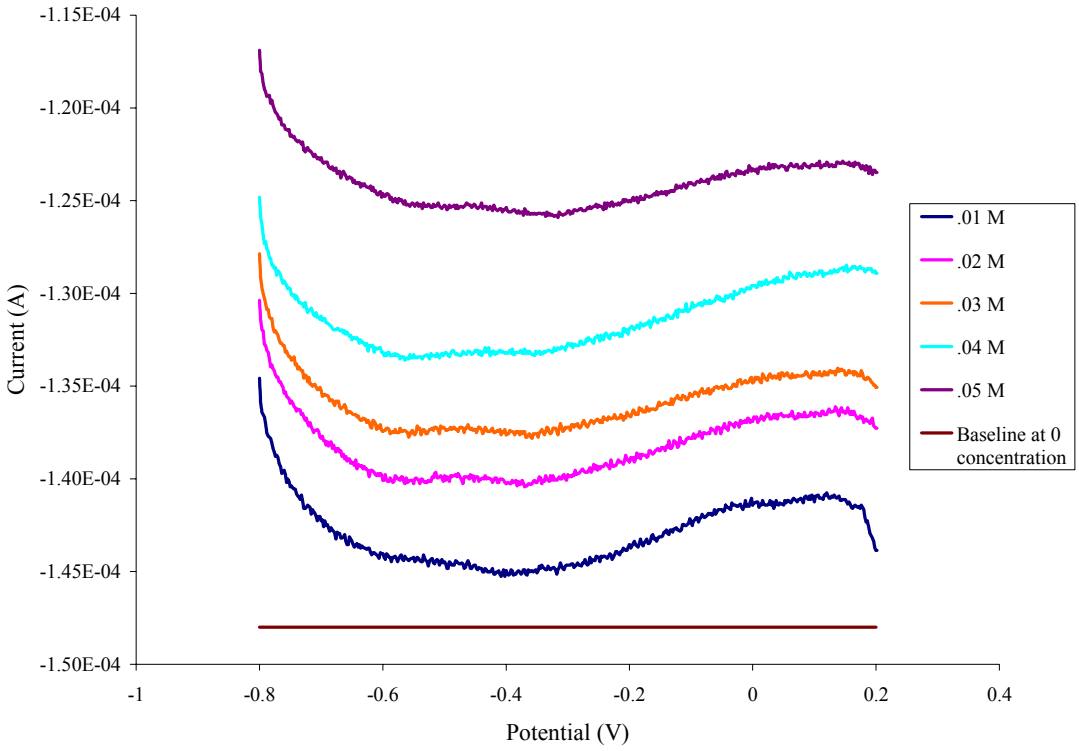

Figure 6.5. Amperometric response of CNT-LOX on Si/ITO substrate in the range of 0.01 M – 0.05 M concentrations of lactic acid.

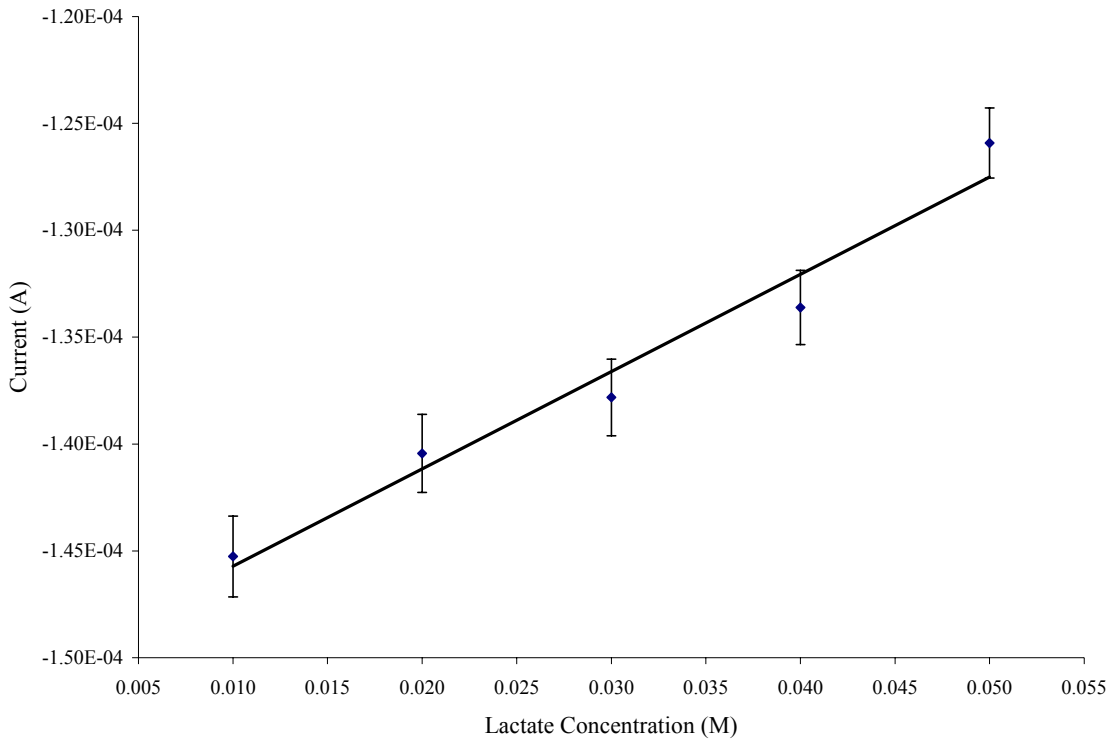

Figure 6.6. CNT-LOX on Si/ITO calibration line.

6.2.2. Functionalized CNTs on Glassy Carbon

When dried on a glassy carbon electrode, the LOX functionalized carbon nanotubes gave a much better response to changes in lactate at lower concentrations. The response curves for this experiment provided better overall resolution (see Figures 6.7 and 6.8). The response current increases linearly with increasing concentration of lactate up to 4 mM, after which steady state was reached. The calibration line was calculated by taking the maximum current reading for each concentration and subsequently plotting that current value versus concentration.

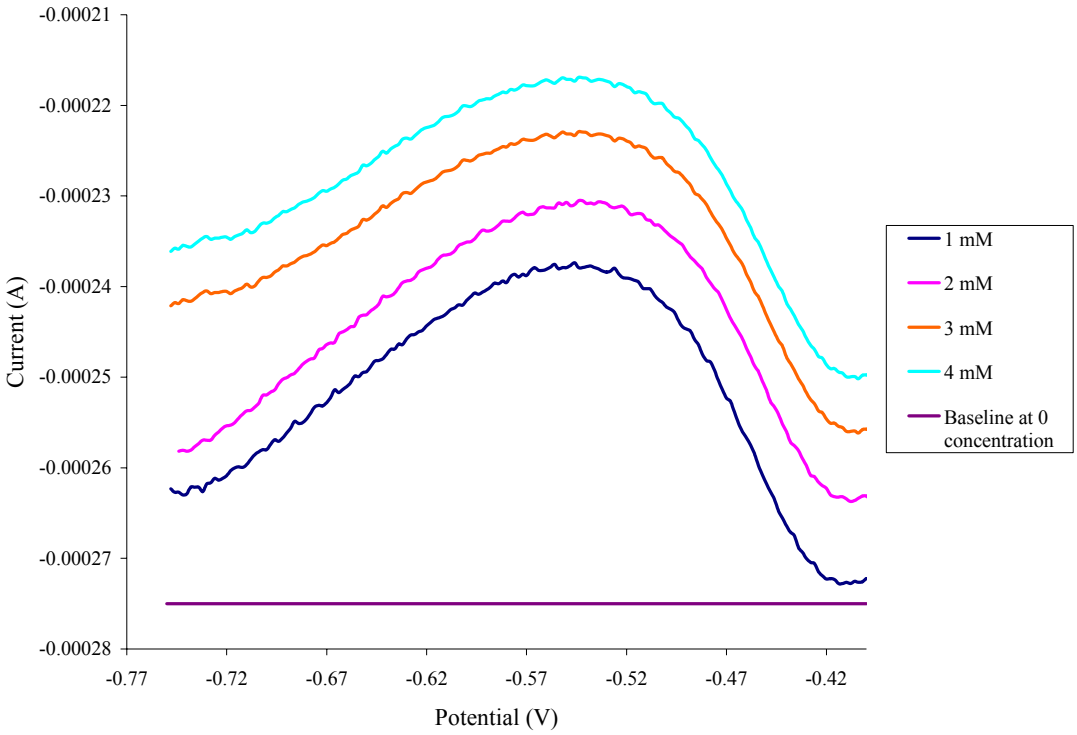

Figure 6.7. Amperometric response of CNT-LOX on glassy carbon in the range of 1 mM to 4 mM concentrations of lactic acid.

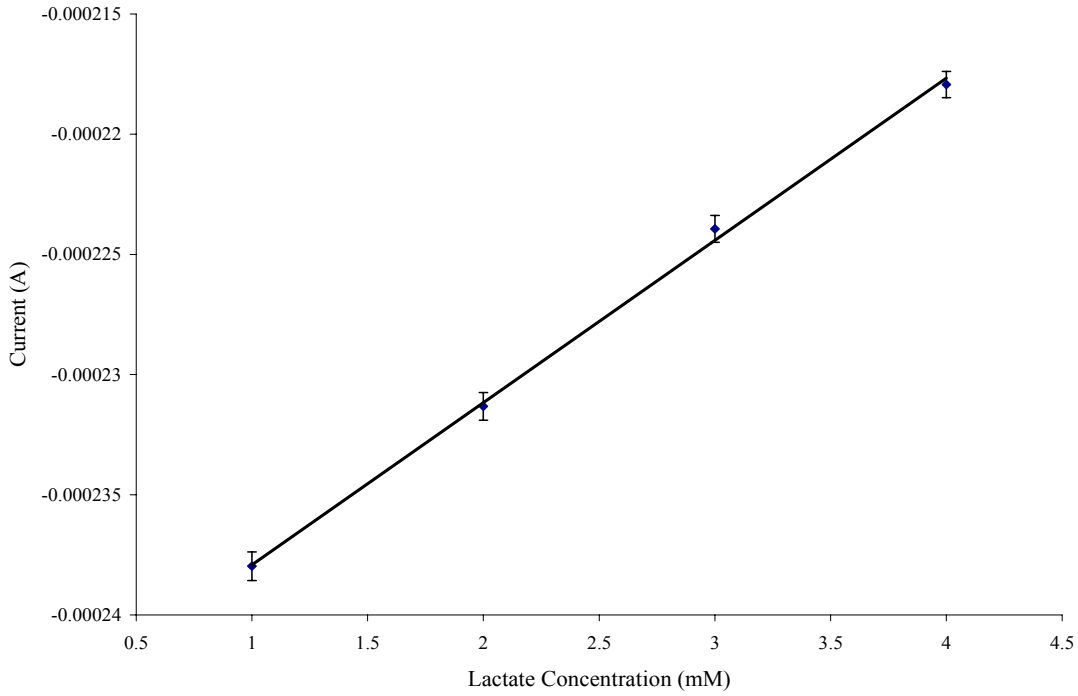

Figure 6.8. CNT-LOX on glassy carbon calibration line.

6.3. Results Review

The following table summarizes the experimental results of the three fabricated electrodes.

Table 6.1. Experimental Summary

Sensor Type	*Functionalization Method*	*Immobilization Method*	*Substrate*	*Electrochemical Technique*	*Detection Limits*
pH Sensor	Chemical	Physical Adsorption	Glassy Carbon	Voltammetry	pH 1-10
Lactate Sensor	Chemical	Physical Adsorption	Si/ITO with Ag Paint	Amperometry	0.01 M to 0.05 M lactate
Lactate Sensor	Chemical	Physical Adsorption	Glassy Carbon	Amperometry	1 mM to 4 mM lactate

Chapter Seven

Summary

Human sweat contains several ions and molecules that, when excreted in abnormal amounts, could be indicative of different internal diseases or problems. In this work, electrochemical sensors designed to target two types of analytes in human sweat were fabricated. Due to their electrical properties, carbon nanotubes were selected as the electrode material for the detection of pH and lactate. They are able to detect low level concentrations and respond well to electrochemical characterization.

Single-walled carbon nanotubes were chemically functionalized to introduce carboxylic acid groups to the sidewalls of the tubes. The ability to functionalize the sidewalls introduced more sites for the adsorption of lactate oxidase onto the tube and consequently allowed more current to be detected. The large amount of LOX immobilized on the nanotube greatly increased the stability of the sensor.

In order to verify that the carbon nanotubes were properly functionalized with carboxylic acid and lactate oxidase FTIR spectra were taken from several samples. The carboxylic acid functionalized nanotubes displayed a broad peak at 2879 cm^{-1} corresponding to the O-H stretch bands and a sharp peak at 1610 cm^{-1} corresponding to the C=O band. The LOX functionalized nanotubes displayed peaks corresponding to the presence of amine groups. N–H bend was shown at 1558 cm^{-1}. N-H out-of-plane bending absorption was also observed at 794 cm^{-1}. C-N stretch occurred at 1190 cm^{-1}.

Carbon nanotubes functionalized with –COOH were extremely sensitive to changes in pH of a phosphate buffer solution. This sensor exhibited a linear response to pH shifts. As expected, a negative shift in voltage was displayed for each increase in pH.

Carbon nanotubes further functionalized with LOX also displayed sensitivity to changes of lactate in a phosphate buffer solution. The CNT-LOX on Si/ITO appeared to show a nearly linear response up to 0.5 M lactate. The silver paint lost its adhesion in the solution at about 0.6 M lactate. This electrode did not display as good of resolution as the CNT-LOX on glassy carbon due to the use of the silver paint. SEM images verified the porosity of the silver paint. Much better resolution was shown on the CNT-LOX glassy carbon electrode. This electrode detected up to 4 mM lactate concentration with a linear amperometric response. Both lactate biosensors showed an increase in current with an increase in lactate concentration.

To overcome the adhesion problem of carbon nanotubes to a substrate surface, future work should include growing the CNTs directly on a silicon substrate. It has been shown that CNTs can be grown via microwave plasma enhanced chemical vapor deposition (MPECVD) and then etched with an acid mixture to eliminate the Si and open the ends of the tubes for functionalization sites [35]. The nanotubes vertically adhered to a thin gold film that was evaporated on one end of the CNTs. It would also be worthwhile to align one single nanotube between two metal contacts to determine if just one CNT would be sensitive enough to respond in changes of pH and lactate.

Another topic for future work would be growth and patterning of an array of CNTs by MPECVD on a substrate. Each separate area of the array could then be

functionalized to specifically detect only one analyte. The sensor array would then be able to simultaneously detect several analytes in human sweat.

References

1. Feynman, R.P., Engineering and Science, 1960.

2. Iijima, S., Nature, 1991. 354: p. 56-58.

3. Gao, G., T. Çagin, W.Goddard, Nanotechnology, 1998. 9: p. 184-191.

4. Olk, C. and J.P. Heremans, J. Mater. Res., 1994. 9(2): p. 259-262.

5. Wildoer, J.W.G., L. Venema, A. Rinzler, R.E. Smalley, C. Dekker, Nature, 1998. 391: p. 59-62.

6. Hafner, J.H., C.L. Cheung and C.M. Lieber, Nature, 1999. 398: p. 761-762.

7. Rinzler, A.G., J.H. Hafner, P. Nikolaev, et al., Science, 1995. 269: p. 1550-1553.

8. Robertson, J., Materials Today, 2004. 7(10): p. 46-52.

9. Guilbault, G.G. and G. Palleschi, Biosensors & Bioelectronics, 1995. 10: p. 379-392.

10. Tamada, J.A., S. Garg, L. Jovanovic, K.R. Pitzer, et al., J. Am. Med. Ass., 1999. 282(19): p. 1839-1844.

11. Horii, I., Y. Nakayama, M. Obata, H. Tagami, Br. J. Dermatol., 1989. 121: p. 587–592.

12. Watanabe, M., H. Tagami, I. Horii, M. Takahashi, A.M. Kligman, Arch. Dermatol., 1991. 127: p. 1689–1692.

13. Nakagawa, N., S. Sakai, M. Matsumoto, K. Yamada, et al., J. Invest. Dermatol., 2004. 122: p. 755-763.

14. Cystic Fibrosis. https://www.walgreens.com/pharmacy/specialpharmacy/specialpharm_cf.jhtml#6

15. Lakard, B., G. Herlem, M. deLabachelerie, W. Daniau, et al., Biosensors & Bioelectronics, 2004. 19: p. 595-606.

16. Hu, C.G., W.L. Wang, S.X. Wang, W. Zhu, Y. Li, Diamond and Related Materials, 2003. 12: p. 1295-1299.

17. Besteman, K., J. Lee, F.G.M. Wiertz, H.A. Heering, C. Dekker, Nano Lett., 2003. 3(6): p. 727-730.

18. Sherigara, B.S., W. Kutner, F. D'Souza, Electroanalysis, 2003. 15: p. 753-772.

19. Dresselhaus, M., G. Dresselhaus, P. Eklund and R. Saito, Physics World, Jan 1998.

20. Weisman, R.B., The Industrial Physicist, 2004. 10(1): p. 24-27.

21. Saito, R., M. Fujita, G. Dresselhaus, M.S. Dresselhaus, Appl. Phys. Lett., 1992. 60(18): p. 2204-2206.

22. Beck, R.D., P. St. John, M.M. Alvarez, F. Diederich, R.L. Whetten, J. Phys. Chem., 1991. 95: p. 8402-8409.

23. Treacy, M.M., T.W. Ebbesen, J.M. Gibson, Nature, 1996. 381(6854): p. 670-680.

24. Wong, E.W., P.E. Sheehan, C.M. Lieber, Science, 1997. 277: p. 1971-1975.

25. Krätschmer, W., L.D. Lamb, K. Fostiropoulos, D.R. Huffman, Nature, 1990. 347: p. 354-358.

26. Guo, T., P. Nikolaev, A.G. Rinzler, D. Tomanek, et al., J. Phys. Chem., 1995. 99: p. 10694-10697.

27. Ren, Z.F., Z.P. Huang, J.W. Xu, J.H. Wang, et al., Science, 1998. 282: p. 1105-1107.

28. Ebbesen, T.W. and P.M. Ajayan, Nature, 1992. 358: p. 220-222.

29. Bethune, D.S., C.H. Kiang, M.S. deVries, G. Gorman, et.al., Nature, 1993. 363: p. 605-607.

30. Kroto, H.W., J.R. Heath, S.C. O'Brien, R.F. Curl, R.E. Smalley, Nature, 1985. 318: p. 162-163.

31. Dresselhaus, M.S., G. Dresselhaus, Ph. Avouris (Eds.), Topics Appl. Phys., 2001. 80: p. 29-53.

32. Balasubramanian, K. and M. Burghard, Small, 2005. 1(2): p. 180-192.

33. Yudasaka, M., R. Kikuchi, T. Matsui, Y. Ohki, S. Yoshimura, Appl. Phys. Lett., 1995. 67(17): p. 2477-2479.

34. Chen, J., M.A. Hamon, H. Hu, Y. Chen, et al., Science, 1998. 282: p. 95-98.

35. Wang, S.G., Q. Zhang, R. Wang., S.F. Yoon, Biochem. Biophys. Res. Comm., 2003. 311: p. 572-576.

36. Liu, J., A.G. Rinzler, H. Dai, J. H. Hafner, et al., Science, 1998. 280: p. 1253-1256.

37. Bahr, J.L., J. Yang, D.V. Kosynkin, M.J. Bronikowski, et al., J. Am. Chem. Soc., 2001. 123: p. 6536-6542.

38. Knez, M., M. Sumser, A.M. Bittner, C. Wege, et al., J. Electroanal. Chem., 2002. 522: p. 70-74.

39. Lane, R.F. and A.T. Hubbard, J. Phys. Chem., 1973. 77: p. 1401-1410.

40. Lane, R.F. and A.T. Hubbard, J. Phys. Chem., 1973. 77: p. 1411-1421.

41. Murray, R.W., Techniques of Chemistry, 1992. 22: p. 1-36.

42. Trau, D. and R. Renneberg, Biosensors and Bioelectronics, 2003. 18: p. 1491-1499.

43. Vidal, J.C., E. Garcia-Ruiz, J. Espuelas, T. Aramendia, J.R. Castillo, Anal. Bioanal. Chem., 2003. 377(2): p. 273 – 280.

44. Xu, J.J., D.M. Zhou, H.Y. Chen, Electroanalysis, 1998. 10(10): p. 713-716.

45. Rahman, Md. A., D.S. Park, Y.B. Shim, Biosensors and Bioelectronics, 2004. 19: p. 1565-1571.

46. Peng, H., L.B. Alemany, J.L. Margrave, V.N. Khabashesku, J. Am. Chem. Soc., 2003. 125: p. 15174-15182.

47. Pavia, D., G.M. Lampman, G.S. Kriz, Introduction to Spectroscopy, 2001.

48. Crow, D.R., ASM Handbook, 1998. 10: p. 187-196.